

THESE
V885
1997
C.2

CONSTRAINTS ON THE TIMING AND CHARACTER OF
PROTEROZOIC DEFORMATION AND METAMORPHISM IN
THE SAN ANDRES MOUNTAINS OF SOUTH-CENTRAL NEW
MEXICO

Geotechnical
Information Center

Kurt Macy Vollbrecht

Department of Earth and Environmental Science
New Mexico Tech
Socorro, New Mexico

Submitted in partial fulfillment for the degree of Master of Science in Geology

August, 1997

**NMIMT
Library
SOCORRO, NM**

3858

Abstract

Proterozoic rocks in the San Andres Mountains of south-central New Mexico show evidence for a single penetrative foliation that developed during one progressive, syn-plutonic, deformational event. This is in contrast to most other Proterozoic exposures in central and northern New Mexico where multiple foliations and deformational events have been described. Much controversy is centered on the timing of the "main" deformational event in New Mexico. In particular, deformation is proposed to have occurred either at 1.6 Ga during the Mazatzal orogeny, or at 1.4 Ga accompanied by widespread plutonism, or at both times. Most studies of the Proterozoic history of southwestern North America have been limited to insights into the timing and character of D_2 deformation, due to a near-universal overprinting of D_1 structures by D_2 . Within the San Andres Mountains this overprinting does not exist and the age and character of D_1 deformation has been determined.

U/Pb dating of igneous zircon from the late-syntectonic Strawberry Peak pluton gives a minimum age for D_1 of ca. 1630 Ma. A maximum age of ca. 1650 Ma is based on U/Pb zircon ages of metavolcanic rocks.

Microstructures, mineral assemblages, and microprobe data indicate that regional deformation occurred at middle- to upper-greenschist facies conditions, whereas microstructures and mineral assemblages proximal to late- and post-tectonic intrusive bodies indicate slightly higher grade conditions. Interpretation of kinematic indicators (S-C fabrics, asymmetric

porphyroclast systems, shear bands) suggest that D_1 was predominately a sinistral strike-slip event with a minor dip slip component. $^{40}\text{Ar}/^{39}\text{Ar}$ thermochronology records reheating to ca. 500°C at 1.4 Ga. Thin section analyses indicate this event was short-lived and was not accompanied by deformation. On the basis of this work, I conclude that 1.6 Ga deformation is recorded throughout New Mexico, whereas the effects of 1.4 Ga deformation appear to be limited to the northern and central portions of the state, possibly due to large-scale heterogeneous strain.

ACKNOWLEDGMENTS

I would like to thank Laurel Goodwin, Paul Bauer, and Dave Johnson for serving on my committee. I benefited greatly during my academic career as a result of the friendship, advice, and support of Laurel, my primary advisor. She has helped me grow as a Geologist and a person and I am fortunate to have had the opportunity to work with her. I would also like to thank Maureen Wilks and Kent Condie, who couldn't be here for the "Grand Finale" but were integral members of my committee nonetheless.

Further support for this project came from Matt Heizler and Kevin Chamberlain who provided thermochronology which was of the utmost importance for this study. Robert Meyers, geologist at White Sands Missile Range, provided much help to insure access to the field site. Financial support from the New Mexico Bureau of Mines and Mineral Resources, the New Mexico Tech Graduate Research Fund, The Geological Society of America, and The Leon Redbone Scholarship Fund was invaluable.

A number of others should be thanked as well for their friendship and input: John Farren (worthy field assistant), John Hall, Joe Marcoline (who taught me the wonders of cooking with yeast products), Steve Ralser, Swami, Dan, Pat, Jeff, and Mic Heynekamp, without whom I would still be trying to retrieve my maps from the depths of my computer. I also would like to thank Debby and Sam and all the other wonderful friends I met at The Box who taught me to "look up, pull hard, and don't let go". Finally I thank my family, especially my mom, who gave me love and support throughout this time, and Koki and Beauregard who unfailingly remind of the joy of life.

TABLE OF CONTENTS

Abstract	i
Acknowledgments	iii
Table of Contents	iv
List of Figures	vi
List of Tables	vii
List of Appendices	viii
List of Plates	ix
Introduction	1
Pervious Work	6
Stratigraphy	9
Metasedimentary Rocks	13
Meta-igneous Rocks	14
Plutonic Rocks	15
Structures	16
Macroscopic Features	16
Post-Proterozoic Structures	21
Microstructure	22
S ₁ Foliation	22
L ₁ lineation	23
Kinematic Indicators	25

Plutonic Rocks: Structure and Contact Relationships	30
Metamorphism	32
Metamorphic Grade	32
Southern Area	33
Northern Area	36
Contact Metamorphism	36
Thermochronology	40
Discussion	45
Deformation	45
Metamorphism	46
Constraint on the timing of deformation and metamorphism provided by igneous history	47
Thermochronology and Regional Implications	49
Conclusion	52
References	54-61
Appendices	62 - 74
Plates	back pocket

LIST OF FIGURES

Figure 1: Proterozoic exposures in southwest North America	2
Figure 2: Structural trends of Proterozoic exposures, New Mexico	4
Figure 3: Proterozoic exposures, San Andres Mountains	8
Figure 4: Detailed map of study area with equal area plots of S ₀	10
Figure 4b: Explanation of map units and symbols	11
Figure 5: Cross-sections	12
Figure 6: Detailed map of study area with equal area plots of S ₁	17
Figure 7: Detailed map of study area with equal area plots of L ₁	18
Figure 8: Sketches of field relationships	20
Figure 9: Photomicrograph of felsic metavolcanic rock	24
Figure 10: Photomicrograph of pelitic schist	26
Figure 11: Photomicrograph of granite mylonite	28
Figure 12: Photomicrograph of garnet porphyroblast in pelitic schist	29
Figure 13: Photomicrograph showing variations in quartz microstructures	37
Figure 14: Photomicrograph of amphibolite	39
Figure 15: ⁴⁰ Ar/ ³⁹ Ar age spectra from muscovite and biotite	43
Figure 16: ⁴⁰ Ar/ ³⁹ Ar age spectra from amphibole	44

LIST OF TABLES

Table 1: Feldspar microprobe data from metavolcanic rock	35
Table 2: Amphibole microprobe data from amphibolite	35
Table 3: Summary of timing and character of Proterozoic deformation in central New Mexico	51

LIST OF APPENDICES

Appendix 1: Brief summary of Proterozoic geochemical data in central New Mexico	62-63
Appendix 2: Petrographic descriptions of Proterozoic rocks from the San Andres Mountains	64-74

LIST OF PLATES

Plate 1: Detailed maps of Proterozoic exposures in the central San Andres

Mountains (1:24,000) back pocket

A) Map showing location of field stations and sample locations

B) Map showing S_0 and outcrop scale fold locations

C) Map showing S_1 and L_1 locations

Introduction

Studies of the Proterozoic history of southwestern North America have addressed deformational events (e.g., Bowring and Karlstrom, 1990 ; Karlstrom and Bowring, 1988; Bauer, 1993; Bauer and Williams, 1994), metamorphic trends (e.g., Grambling et al., 1988; Grambling et al., 1989), and geochemical trends (e.g., Condie, 1986). The focus of these studies has generally been on Proterozoic rocks of the transition zone of central Arizona and northern New Mexico, with little emphasis on deformation and metamorphism of similar age rocks in southern New Mexico. A better understanding of the complex metamorphic and tectonic processes active during the Proterozoic assembly of the North American continent has been gained through the synthesis of these previous studies with detailed structural and metamorphic work in the San Andres Mountains of southern New Mexico.

Accretion of Proterozoic terranes to the Archean Wyoming province proceeded broadly from NW to SE during the Yavapai orogeny (1.7 Ga), and the Mazatzal orogeny (1.65-1.60 Ga) (Bowring and Karlstrom, 1990; Bauer and Williams, 1994) (Fig. 1). The timing of the major tectonic event in northern New Mexico has been widely debated and two models have been proposed. The first model, based on structural analysis, metamorphic trends, and U/Pb zircon ages of deformed and undeformed igneous rocks, suggests that major deformation and metamorphism occurred at 1.6 Ga, with reheating and localized deformation along pluton margins accompanying widespread

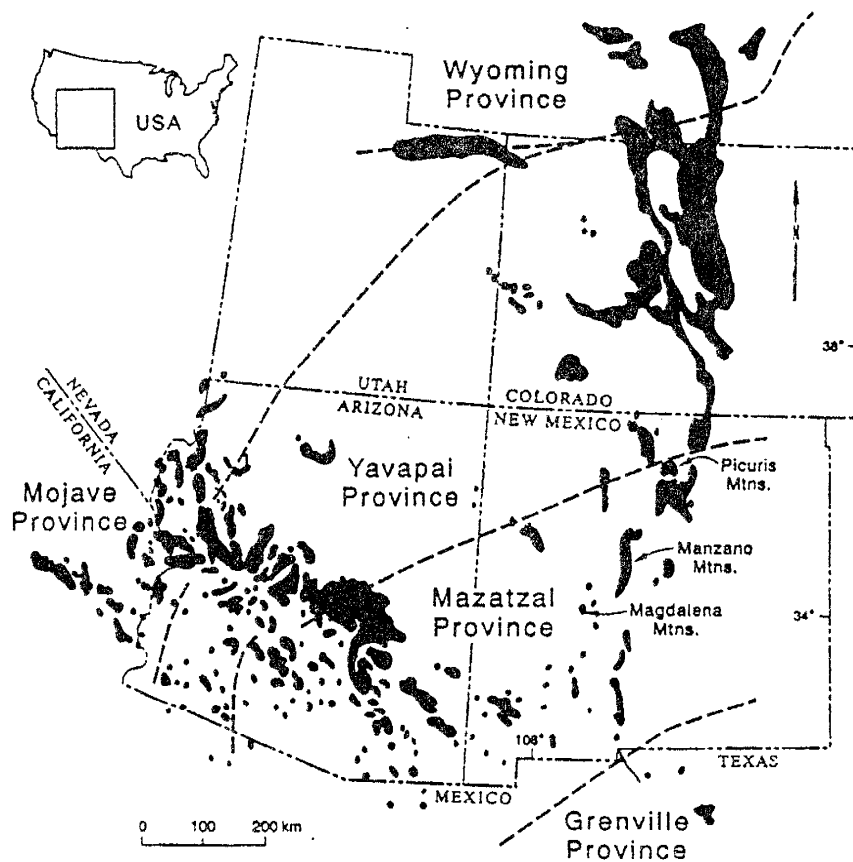


Figure 1: Generalized map of Proterozoic exposures in the southwestern United States showing approximate boundaries of orogenic provinces. Modified from Bowring and Karlstrom (1990) and Bauer and Williams (1994).

plutonism at 1.4 Ga. In the Picuris Mountains of northern New Mexico (Fig. 2), 1.65 Ga deformation is postulated based on U/Pb zircon dates on the strongly deformed, syntectonic Rana quartz monzonite and Puntiajado granite porphyry (ca. 1680 Ma) (Bauer, 1993). Within the Magdalena Mountains of central New Mexico (Fig. 2), D_1 deformation is tightly constrained by cross-cutting relationships between strongly deformed metavolcanic rocks (1664 ± 3 Ma) and the undeformed Magdalena granite (1654 ± 1 Ma) (Bauer and Williams, 1994).

A second model, based on structural analysis, metamorphic trends, and $^{40}\text{Ar}/^{39}\text{Ar}$ thermochronology suggests that major deformation and metamorphism occurred at 1.4 Ga. This model is supported by $^{40}\text{Ar}/^{39}\text{Ar}$ ages on: 1) S_2 -defining hornblendes (1406 ± 16 Ma) which crosscut an older foliation from the Capilla Peak area of the Manzano Mountains (Fig. 2) (Marcoline, 1996); 2) hornblende from the Manzano Mountains (1438 ± 5 Ma) interpreted to represent timing of regional ductile extension (Thompson et al., 1991); and 3) hornblende (1394-1398 Ma) from metavolcanic rocks in the Cimarron Mountains (Fig. 2) interpreted to represent cooling shortly after metamorphism and deformation (Grambling and Dallmeyer, 1993). Furthermore, evidence for late-syntectonic emplacement (L. Goodwin, unpublished data) of the ca. 1450 Ma Peñasco quartz monzonite (Bauer, 1993) and ca. 1450 Ma U/Pb ages of metamorphic minerals from the Tusas and Picuris Mountains (Lanzirotti, 1996) support models calling for deformation

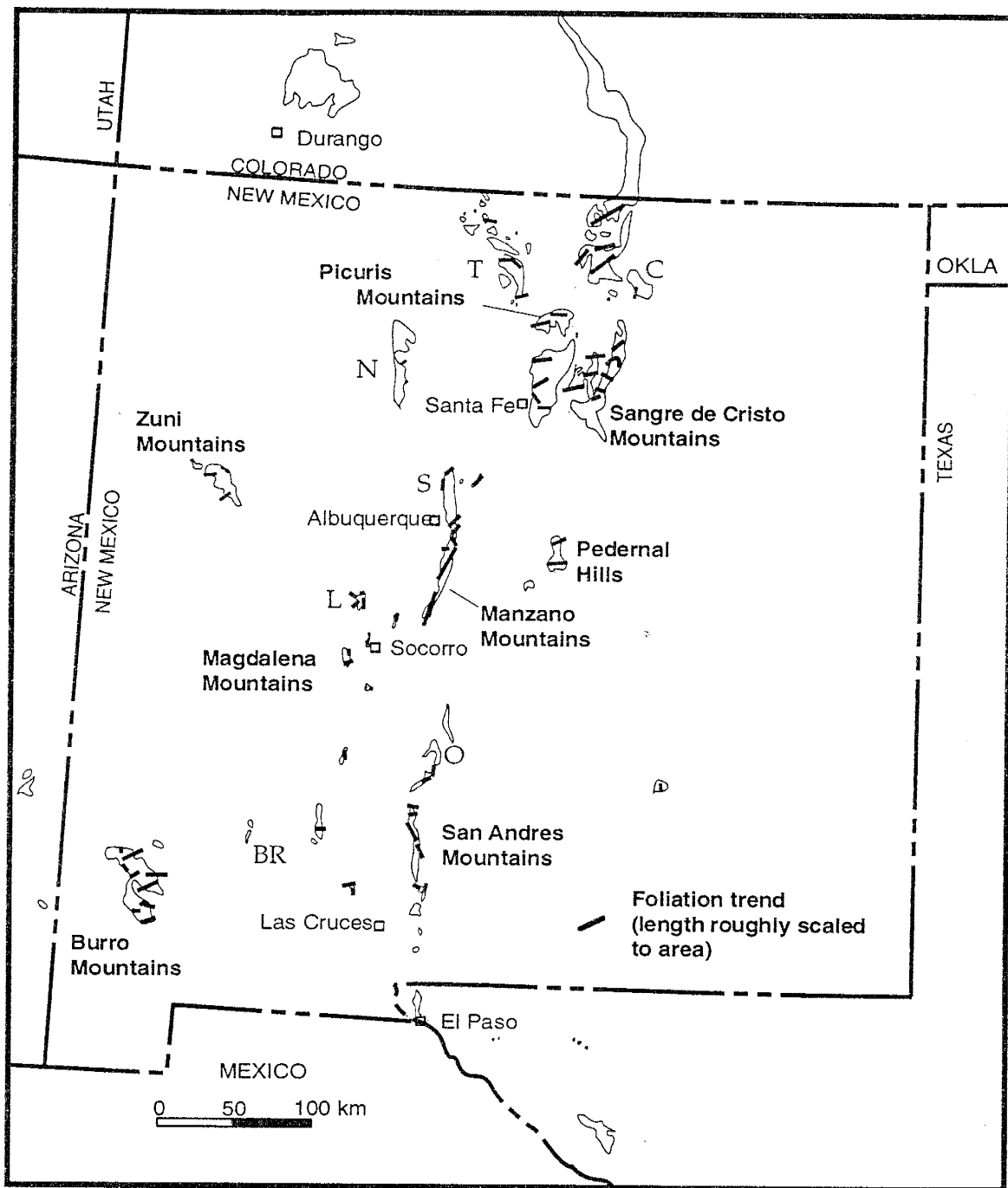


Figure 2: Compilation by Steve Ralser, Laurel Goodwin, and Maureen Wilks of structural data for Precambrian exposures in New Mexico. Data from Condie and Budding (1979), Bauer and Williams (1985, 1989, 1994), Bauer et al. (1993), Mawer and Bauer (1989), Goddard (1966), Hewitt (1959), Robertson and Condie (1989), Roths (1991), Williams (1991), and Woodward (1987). Additional data in northern New Mexico and the Burro Mtns compiled from USGS geologic maps. BR - Black Range, C - Cimarron Mtns, L - Ladrones, N - Nacimiento Mtns, O - Oscura Mtns, S - Sandia Mtns, T - Tusas Mtns.

at 1.4 Ga. In all cases of 1.4 Ga deformation the event is known to be at least D_2 .

These data suggest that Proterozoic rocks in New Mexico record not just one, but two deformation events including 1.6 Ga D_1 deformation recorded throughout the state, and younger 1.4 Ga D_2 deformation recorded in the well-studied northern and central portions of the state where evidence for multiple episodes of deformation is common. Distribution of areas which show evidence for multiple deformation events and those with evidence for a single episode of deformation can be loosely correlated with the distribution of structural trends in New Mexico, discussed below.

Within extensively studied areas of southwestern North America, foliations predominantly strike E to NE and the age of juvenile crust decreases to the SE. This is consistent with a model which calls for simple progressive NW to SE accretion during orogenesis. However, in parts of New Mexico, structural trends do not parallel these regional trends. Proterozoic exposures in northern, eastern, and western New Mexico are characterized by E- to ENE-striking tectonic foliations (Fig. 2). Structural analyses in these areas have demonstrated similar histories of N- to NNW- directed ductile thrusting and N-S shortening (e. g., Bauer and Williams, 1985; Williams, 1991). This structural history is broadly consistent with the regional history.

Proterozoic exposures in central New Mexico are anomalous in that the dominant foliation strikes NNE and NNW (Fig. 2). The San Andres Mountains of south-central New Mexico represent one of the largest

exposures of Proterozoic rocks within the Central Domain (Fig. 2). These mountains are located on the western edge of the Tularosa Basin, within the White Sands Missile Range. Very little work has been completed in this structurally unique exposure of Proterozoic rocks, due mainly to severely restricted access. This paper presents the results of detailed field mapping, structural analysis, and thermochronology of an area that contains all of the elements necessary to fully characterize the deformational history of this domain. These elements include areas dominated by a NE-striking foliation, areas dominated by a NW-striking foliation, and deformation-bracketing plutons. The results of field and petrographic studies indicate that the dominant foliation in the San Andres Mountains is S_1 , whereas in northern New Mexico the dominant foliation is at least S_2 . Deformation occurred at middle to upper greenschist facies conditions, similar to conditions of D_1 deformation in the Magdalena Mountains (Bauer and Williams, 1994) and Manzano Mountains (Marcoline et al., 1996). This is in contrast to amphibolite facies conditions of D_2 deformation in northern and central New Mexico (e.g. Grambling and Dallmeyer, 1993; Marcoline et al., 1996). Field relationships and thermochronology indicate that D_1 deformation and metamorphism occurred at ca. 1650 Ma in the San Andres Mountains.

Previous Work

Kottlowski (1955, 1959) and Kottlowski et al. (1956) provided the first descriptions of Proterozoic rocks in the San Andres Mountains. More recent

studies include geochemical studies and reconnaissance mapping by several workers (Condie and Budding, 1979; Condie, 1986, Alford, 1987), and limited structural analysis in two areas, Dead Man Canyon and Little San Nicolas Canyon (Fig. 3) (Roths, 1991). A summary of previous geochemical studies is given in Appendix A.

Condie and Budding (1979) produced a generalized geologic map of Precambrian exposures in the San Andres Mountains. They focused on the petrography and geochemistry of Precambrian rocks over a large area of central and south-central New Mexico, rather than on the structural geology of any single range. They also provided detailed lithologic descriptions of metasedimentary rocks (phyllite, schist, quartzite), mafic and siliceous metaigneous rocks (amphibolite, metadiabase, metarhyolite), and plutonic rocks from the San Andres Mountains. Two of the plutons described by Condie and Budding are within the study area; the medium-grained Strawberry Peak granite and the medium- to coarse-grained Capitol Peak quartz monzonite. They made no mention of the strongly deformed pluton (herein called the Boki granite) that is exposed along the eastern margin of my map area (Fig. 4 and 5). In addition, I have mapped a sequence of pelitic schist and quartzite between Ash Canyon and Workman Canyon where Condie and Budding (1979) showed a gneiss (Fig. 4 and 5).

Alford (1987) focused on geochemistry, stratigraphic relationships between metaigneous and metasedimentary rocks, and interpretation of depositional and tectonic environments in the Hembrillo Canyon area.

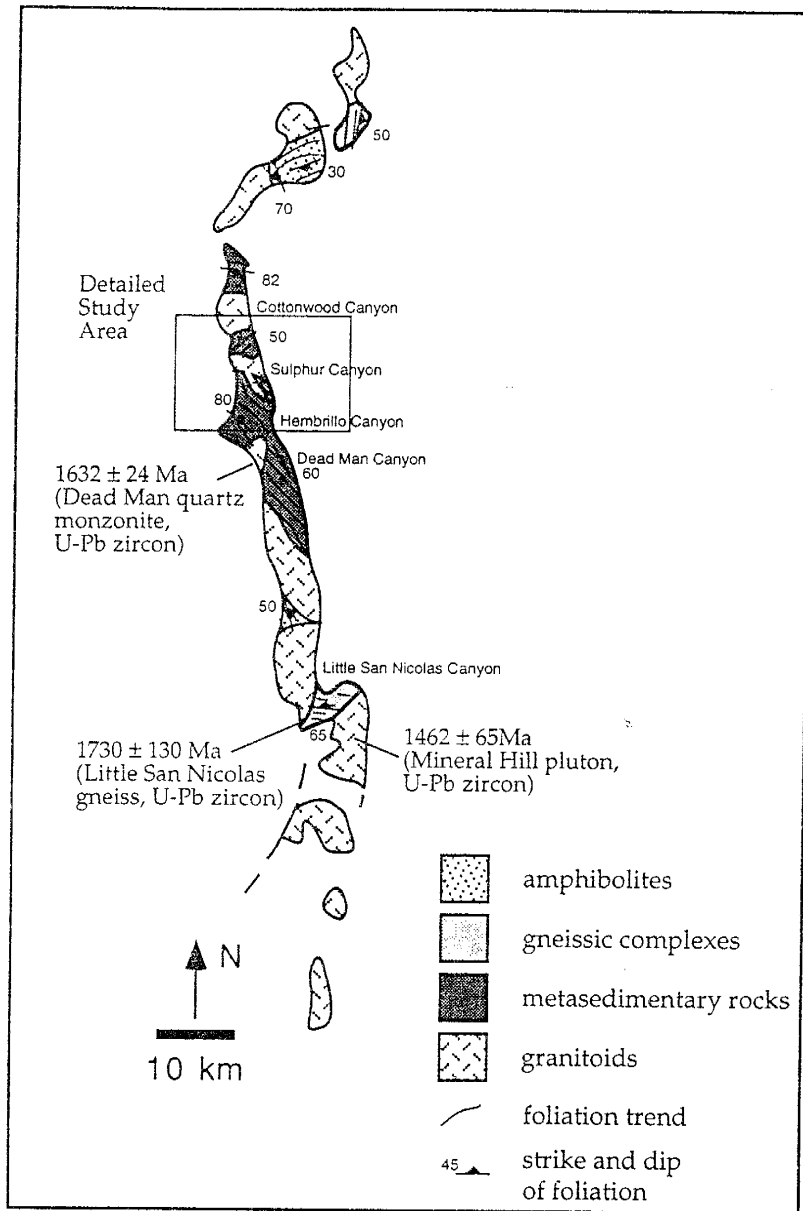


Figure 3: Generalized geologic map of the San Andres Mtns showing Proterozoic exposures and detailed study area. Modified from Condie & Budding (1979) and Condie (1981), with data added from Roths (1991) and current study.

Although he added some detail to Condie and Budding's map, several key structural and lithologic elements were overlooked. My map shows relocated major lithologic contacts and reveals a map-scale syncline north of Hembrillo Canyon.

Roths (1991) presented evidence for three episodes of deformation at two locations within the southern San Andres Mountains, in Little San Nicolas Canyon and Dead Man Canyon (Fig. 3). Reconnaissance field work in the Dead Man Canyon area confirms the existence of a NW-trending foliation (S_2 of Roths), yet no evidence of multiple deformation events was observed. U-Pb analysis of zircon from a pluton in Dead Man Canyon containing the NW foliation reveals a maximum age for deformation of 1632 ± 24 Ma, whereas zircon from an unfoliated pluton in Little San Nicolas Canyon indicate a minimum age for deformation of 1462 ± 67 Ma (Roths, 1991).

Stratigraphy

Metamorphic rocks from the central San Andres Mountains are dominantly schist, phyllitic schist, metaconglomerate, and quartzite, with lesser amounts of felsic and mafic metavolcanic rocks. The supracrustal package is composed of ~ 50 % schistose metasedimentary rocks, ~30 % quartzite, and ~20 % metavolcanic rocks. The supracrustal rocks are intruded by felsic and mafic igneous rocks which range from virtually undeformed to strongly deformed. Detailed lithologic descriptions of these rocks are in Condie (1986) and Alford (1987). The following sections provide brief

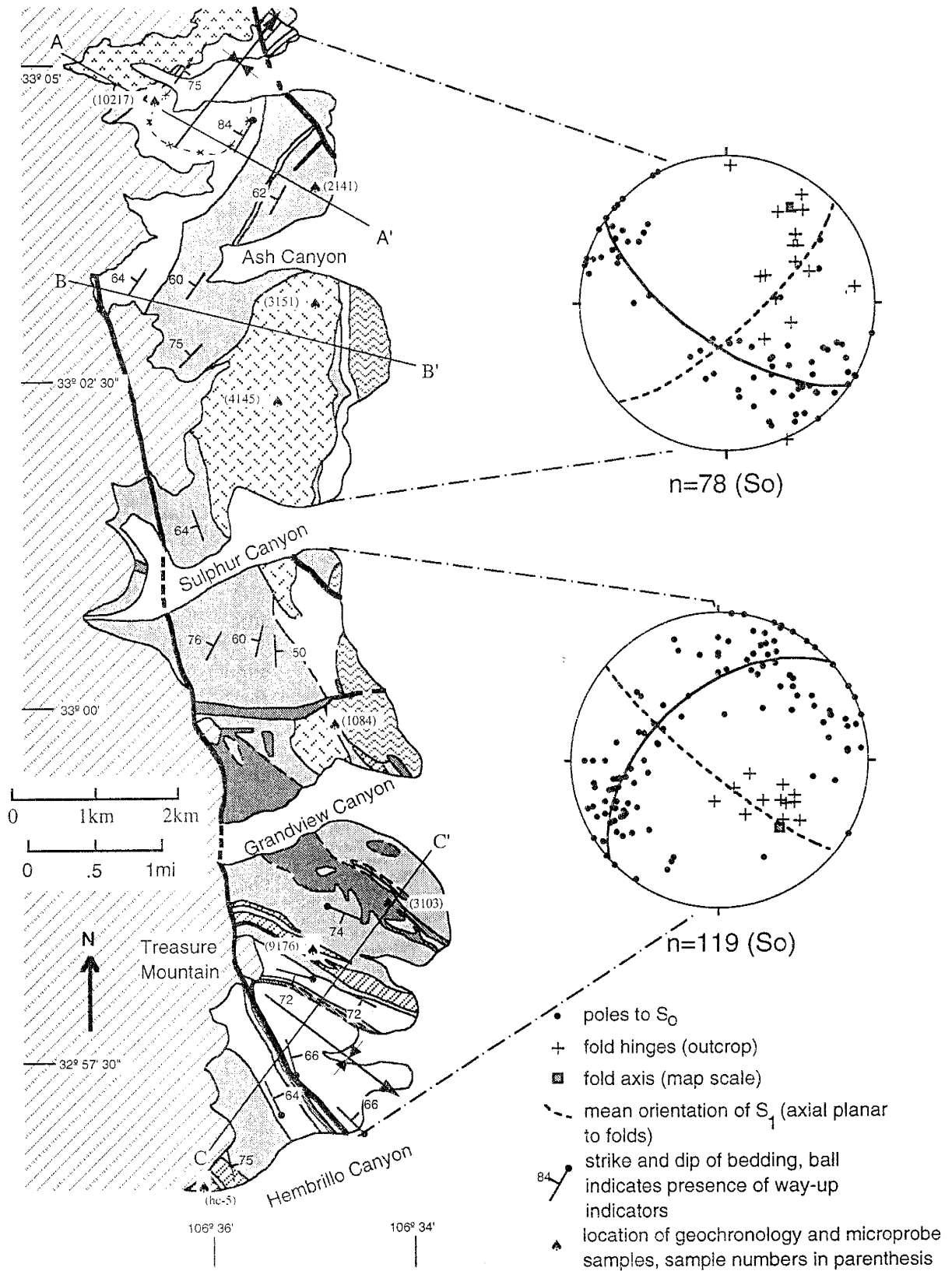


Figure 4: Geologic map of central San Andres Mountains with lower hemisphere equal area plots of bedding (S_0) and locations of cross sections. Great circle girdles containing poles to bedding are shown as solid lines on plots.

Explanation

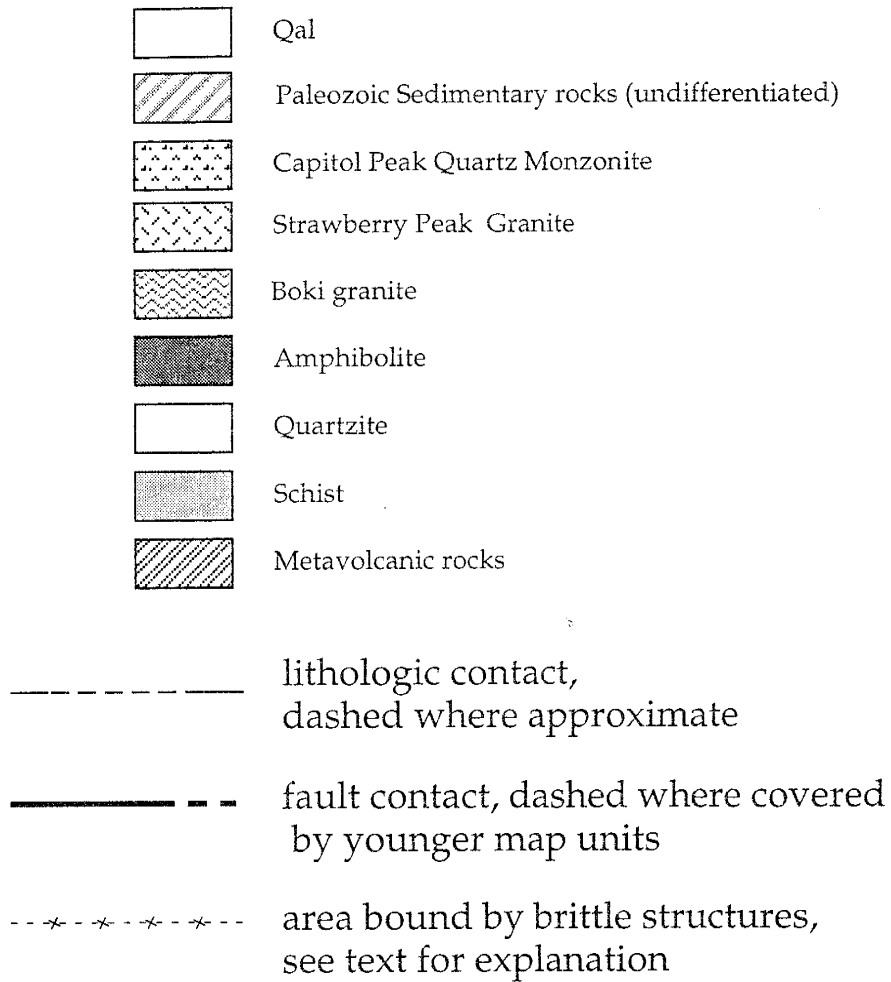


Figure 4b: Explanation of map units shown in figures 4, 5, 6, and 7. Contacts shown here apply to figures 4, 6, and 7.

descriptions of the rock types observed in the current study. Detailed petrographic descriptions completed for this study are given in Appendix B.

Metasedimentary rocks

Metasedimentary rocks in the central San Andres Mountains vary in composition from north to south. This is likely the result of along-strike differences in the original sedimentary sequence. On the basis of these trends the supracrustal rocks can be separated into a southern area stretching from Hembrillo Canyon to Grandview Canyon, a central area from Grandview Canyon to Ash Canyon, and a northern area from Ash Canyon to Workman Canyon (Fig. 3).

In the southern area arkosic schists interbedded with minor quartzite include green to brown phyllitic schists, quartzofeldspathic mica (white mica \pm biotite) schist, and strongly foliated metaconglomerate. Quartzites with well preserved sedimentary structures including crossbedding, graded beds, and scour marks are found in a relatively homogeneous band just north of Hembrillo Canyon.

Metasedimentary rocks in the central area are dominated by arkosic schists and strongly foliated metaconglomerate similar to those found in the southern area. Paleozoic rocks to the west cover the thick quartzites that are exposed in the northern and southern areas.

In the northern area, arkosic schists are less abundant. Pelitic units become increasingly abundant north of Ash Canyon. The latter include

garnet- and andalusite-bearing muscovite schists just north of Strawberry Peak. A homogeneous band of quartzite that correlates with the quartzite north of Hembrillo Canyon outcrops in the northwest portion of the area.

Meta-igneous rocks

Metavolcanic rocks are exposed in the area between Treasure Mountain and Grandview Canyon as conformable layers within the metasedimentary sequence (Figs. 4 and 5). The metavolcanic rocks range from pink to gray, with relict quartz and plagioclase phenocrysts and lenses of fine grained quartz and K-feldspar interpreted as relict fiammé. These lie in a fine-grained matrix of quartz and feldspar with varying amounts of biotite, white mica, and epidote. A protolith of volcanic tuff is indicated by such textures.

A number of amphibolites exist in the southern portion of the study area as well. Contacts with the surrounding sediments are both concordant and discordant. Ophitic and subophitic textures are observed in some concordant amphibolites; structures resembling columnar jointing and pillows are observed in others (Condie and Budding 1979; Alford, 1987). The concordant amphibolites are therefore interpreted to be both sills and flows. A large amphibolite complex northeast of Treasure Mountain exhibits discordant contacts and is likely a dike complex, composed of a number of small intrusive bodies.

Plutonic rocks

The three felsic intrusive bodies mapped in the study area include the, informally named Boki pluton, the Strawberry Peak pluton, and the Capitol Peak pluton (Fig. 4). Brief descriptions of these plutons are given below, while relationships indicating the relative timing of deformation and intrusion are detailed in a following section.

The Strawberry Peak and Boki plutons were originally, and incorrectly, mapped as part of the same intrusive body (Alford, 1987). The Boki pluton is a medium-grained granite with a well-developed tectonic foliation. It is composed dominantly of quartz and K-feldspar with lesser amounts of plagioclase and biotite. The Boki pluton lies along the eastern edge of the study area and is covered to the east by Quaternary alluvium (Fig. 4, and Fig. 5, section B-B').

The Strawberry Peak pluton is a medium-grained, two mica (biotite - muscovite), equigranular granite. Quartz, plagioclase and K-feldspar are present in equal amounts. The Strawberry Peak pluton is centrally located in the study area and marks the transition between NE- and NW- striking fabrics (Figs. 4, 5, 6, and 7).

The Capitol Peak pluton is a medium- to coarse-grained quartz monzonite containing euhedral plagioclase and K-feldspar laths up to 4 cm in length. Plagioclase exhibits concentric zoning and quartz grains are equant. This pluton lies at the north end of the study area, north of Workman

Canyon and has been mapped up to 40 km to the north (Fig. 4 and Fig. 5, section A-A') (Condie and Budding, 1979).

Structures

The ductile features associated with Proterozoic mid-crustal deformation exhibit a progressive change in orientation and character from north to south. The following sections provide detailed descriptions of the ductile features and an overview of post-Proterozoic brittle features.

Macroscopic Features

The dominant structures in Proterozoic rocks of the central San Andres Mountains are a doubly plunging syncline spanning the entire length of the study area and a penetrative axial planar cleavage (S_1) (Figs. 4 and 6). The map-scale fold in bedding (S_0) is best exposed in the southern portion of the study area from Hembrillo Canyon north to Treasure Mountain (Fig. 5, section C-C'). In this area a thick quartzite unit is cylindrically folded about a fold axis plunging 52° toward 125° (Fig. 4, lower plot). The orientation of abundant, well preserved, relict trough crossbeds indicates that the sequence is upright. North of Ash Canyon the map scale fold axis plunges 43° toward 039° (Fig. 4, upper plot).

Intrafolial folds in cm-thick schist layers in quartzite are upright and tight to isoclinal, whereas folds within meter- to several-meter-thick quartzite beds are generally open and upright (Fig. 8a and 8c). Throughout the study

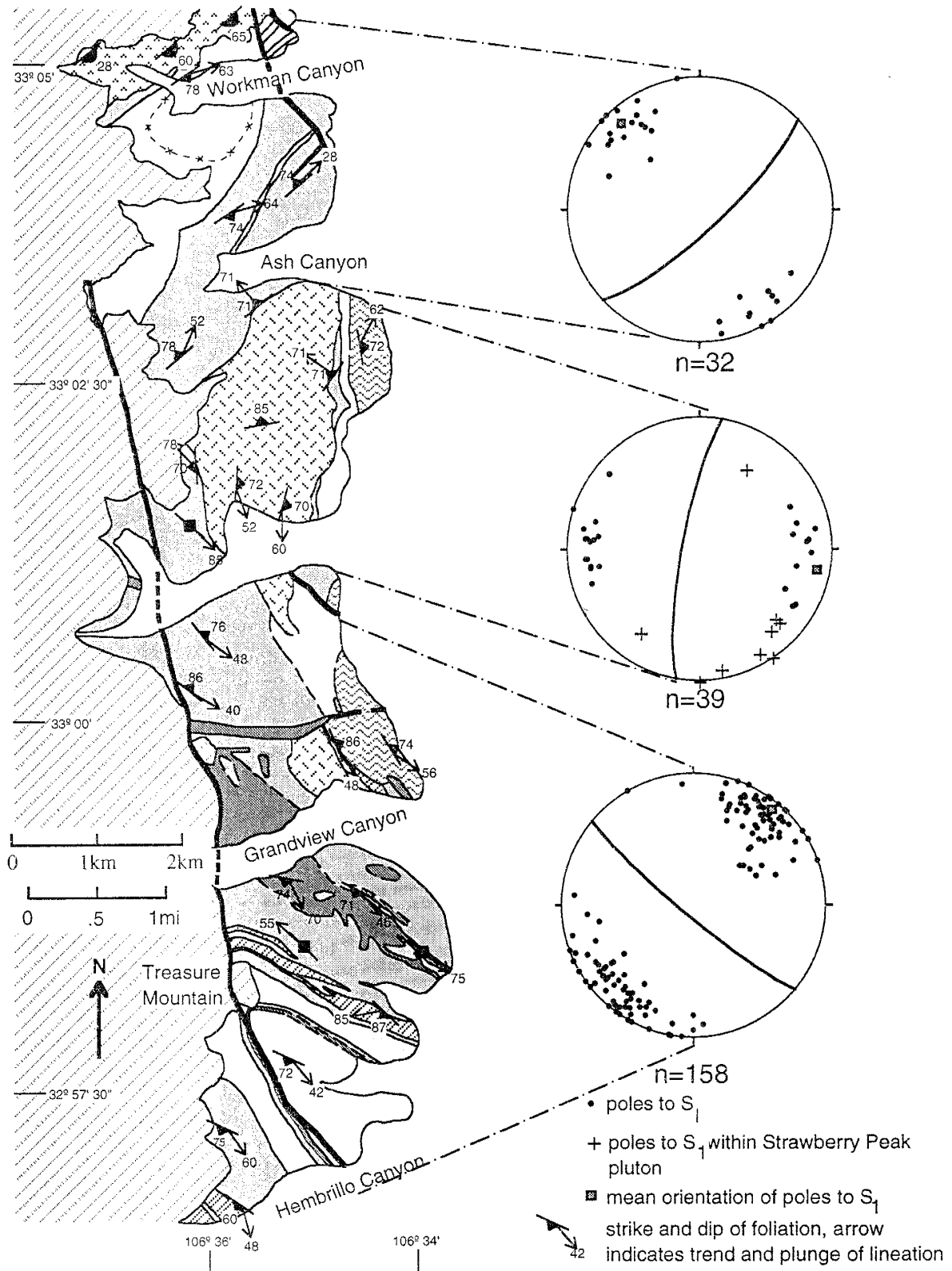


Figure 6: Geologic map of central San Andres Mountains with equal area plots of foliation (S_1). The mean orientations of S_1 in different domains are shown as solid lines on plots.

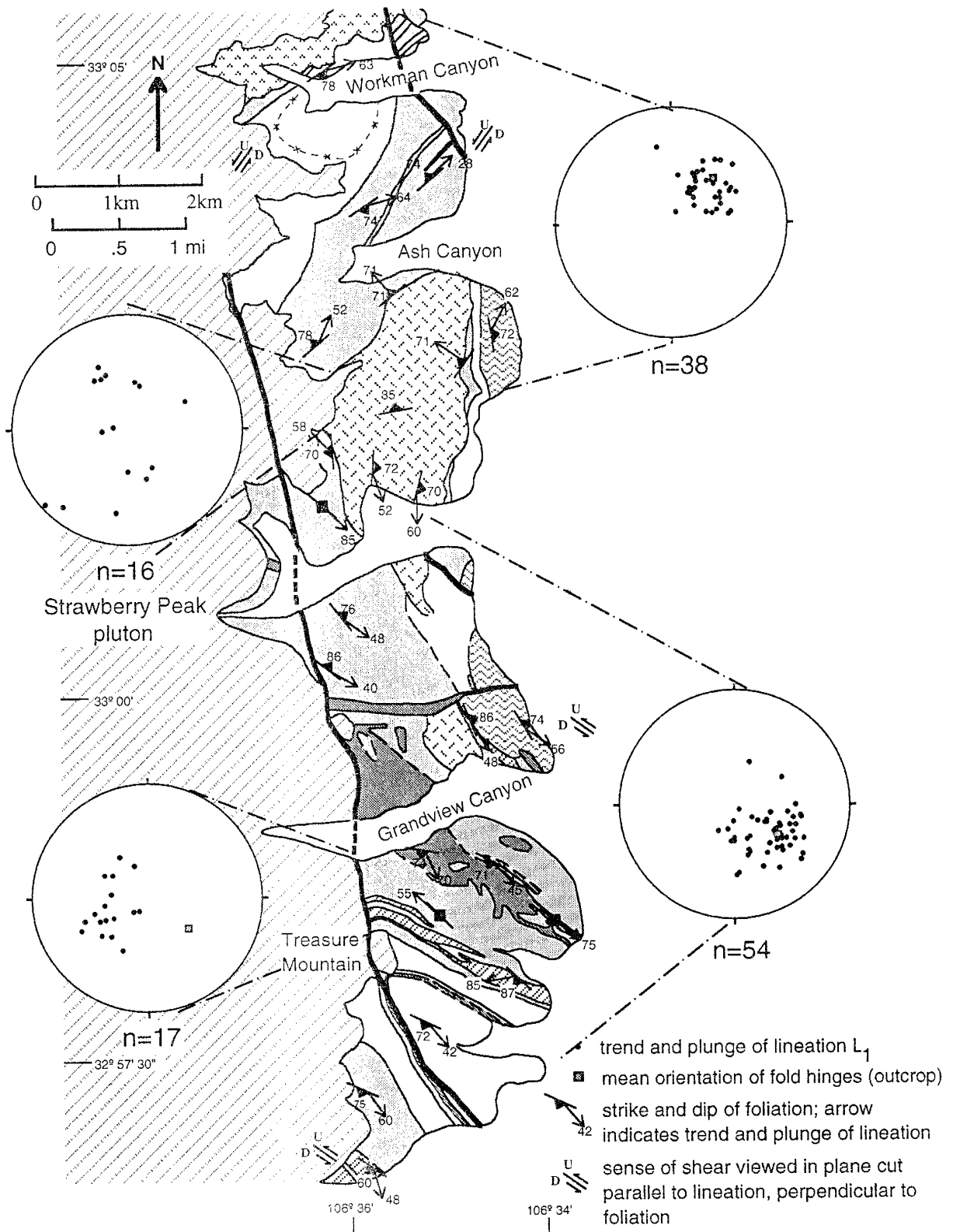


Figure 7: Geologic map of central San Andres Mountains showing domainal distribution of lineation and sense of shear.

area, outcrop-scale fold hinges are subparallel to the map-scale structure (Fig. 4). Within areas dominated by less competent schist and phyllite, fold geometries are much less consistent, ranging from isoclinal intrafolial folds to disharmonic ptygmatic folds (Fig. 8b). Symmetrical chevron folds with 1-2-cm-long limbs were found in one location, in a schist just north of Treasure Mountain. On all scales, folds are cut by a penetrative axial planar cleavage (S_1). S_1 is dominantly parallel to bedding to slightly oblique to bedding except in the hinges of folds.

S_1 exhibits a progressive change in orientation from NW-striking in the south to NE-striking in the north. Equal area plots of relatively homogeneous domains clearly show this change (Fig. 6). Within the southern portion of the study area, from Hembrillo Canyon north to Sulphur Canyon, S_1 strikes, on average, approximately N50W. In the central portion of the study area, from Sulphur Canyon to Ash Canyon S_1 strikes approximately N-S. An exception to this is found in the Strawberry Peak pluton where discrete shear zones exhibit disparate orientations (cross symbols, central plot in Fig. 6). North of Ash Canyon the mean orientation of S_1 is approximately N50E. Throughout the study area the dip of S_1 ranges from E to W within 20° of vertical.

A poorly developed to well-developed mineral lineation (L_1) also exhibit a domainal distribution of orientations (Fig. 7). In the area south of Sulphur Canyon, L_1 plunges moderately to the SE, except in metavolcanic rocks and schists just south of Grandview Canyon, where L_1 plunges

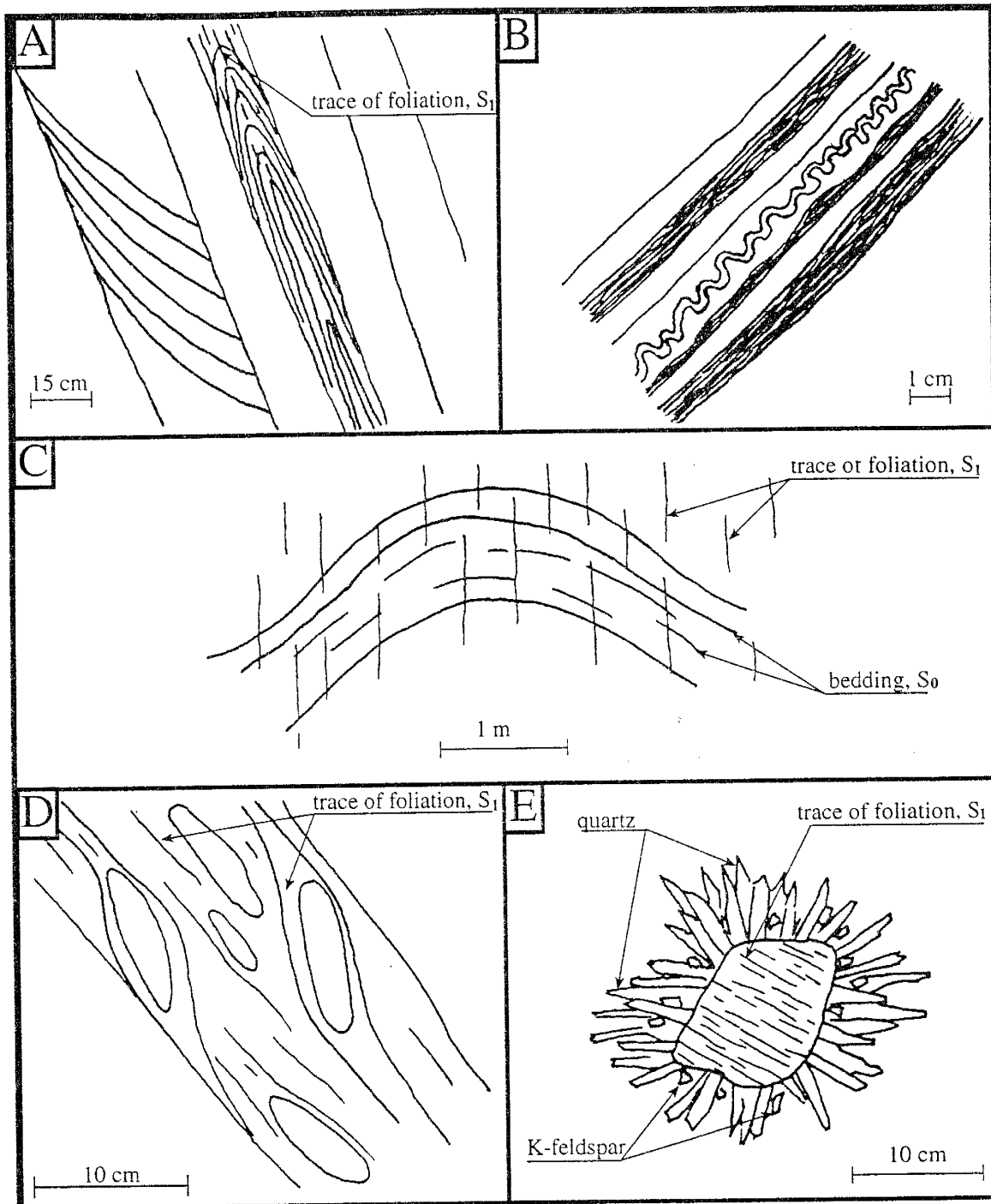


Figure 8: Sketches showing field relationships (photography was prohibited on White Sands Missile Range) A) Intrafolial folding of less competent biotite schist within quartzite beds with relict trough crossbeds. View is perpendicular to S_1 and oblique to L_1 . S_1 is axial planar to fold. B) Ptygmatic folding of quartz rich layer interbedded with alternating muscovite- and biotite-rich layers. Plane of sketch is perpendicular to S_1 (S_1 parallel S_0) and L_1 . C) Open fold in quartzite layers. S_1 is axial planar to fold. Plane of sketch is perpendicular to S_1 and fold axis. D) Elongate pebbles in metaconglomerate. Rare "stepping" of foliation around pebbles is consistent with sinistral sense of shear. Plane of sketch is perpendicular to S_1 and parallel to L_1 . E) Xenolith of schist surrounded by radiating crystals of quartz and K-feldspar in pegmatite south of Workman Canyon.

moderately to steeply west (Fig. 7, lower left plot). The boundaries of this unique domain parallel lithologic contacts, with an amphibolite complex to the NE and thick quartzites to the SW.

Orientations of L_1 within the variably deformed Strawberry Peak pluton are highly variable, reflecting the change in orientation of foliations within discrete shear zones and contact zones (Fig. 7, upper left plot). In the northern portion of the study area, however, L_1 plunges moderately and consistently to the NE. L_1 throughout the study area is generally subparallel to fold hinges, with the exception of the anomalous area between Grandview Canyon and Treasure Mountain where L_1 is nearly normal to the mean orientation of fold hinges (Fig. 7, lower left plot).

The progressive change in orientation of S_1 from NE-striking in the north to SE-striking in the south, coupled with the mean orientation of folds north and south of the Strawberry Peak pluton, indicates that the entire supracrustal package, including the large syncline, is folded about a steeply east dipping, E-W trending fold axis. Adjacent to the Strawberry Peak pluton lineations steepen, becoming sub-parallel to the dip direction of S_1 .

Post-Proterozoic Structures

Several brittle structures are evident within the study area. The most prominent is a , east-up, steeply east-dipping fault along the western portion of the field area (Fig. 4 and Fig. 5). Seager (1981) describes similar faults in the southern San Andres Mountains which, based on field relationships

including faulting of Cretaceous sediments that are overlain by Eocene volcanic andesites, are thought to be Laramide in age. West-down, reverse movement is also consistent with Laramide faulting. Offsets of gently west-dipping Paleozoic sedimentary rocks and the Proterozoic syncline near Treasure Mountain are small. Orientations of Proterozoic structures are similar on either side of the fault.

Range-bounding normal faults are exposed along the eastern margin, adjacent to, and buried by, Quaternary alluvium. Normal faulting has resulted in tilting of Proterozoic strata approximately 10° to the west, judging from the orientations of overlying Phanerozoic rocks.

Microstructure

S₁ Foliation

S₁ is best developed in areas dominated by schist and phyllitic schist, where the foliation is defined by the preferred alignment of phyllosilicate phases: dominantly muscovite with lesser amounts of biotite and chlorite. S₁ is defined in quartzites by the shape-preferred orientation of elongate quartz grains and minor amounts of muscovite. Alternating mica-rich and quartzofeldspathic bands define S₁ within metavolcanic rocks (Fig. 9). Preferred alignment of biotite and elongate amphibole crystals define S₁ in amphibolites.

L₁ Lineation

Within metavolcanic rocks, the mineral lineation is defined by elongate pods of very fine-grained, polycrystalline K-feldspar and quartz with axial ratios up to 10:1. Also present are elongate, locally extended lenses of epidote in metarhyolites near Hembrillo Canyon where epidote replacement of feldspar is common. Feldspar porphyroclasts are locally boudinaged parallel to L₁ with quartz infilling necks between boudins (Fig. 9). L₁ in amphibolites is defined by elongate and locally boudinaged sphene and amphibole with axial ratios up to 10:1. Within the strongly deformed Boki granite, the mineral lineation is defined by elongate pods of polycrystalline quartz and K-feldspar. Pelitic schists found in the northern portion of the study area have L₁ defined by andalusite with axial ratios up to 5:1 and mm-scale lenses of polycrystalline biotite (Fig. 10). Within a continuous band of metaconglomerate that outcrops south of Sulphur Canyon to Ash Canyon, elongate pebbles define a consistent lineation lying in the plane of S₁. Pebbles range from 1 cm to 10 cm in length and are equant perpendicular to lineation with axial ratios ranging from 2:1 to 5:1 parallel to lineation. The extension of feldspar porphyroclasts, sphene, and amphibole, and the presence of stretched pebbles indicate that L₁ is a stretching lineation.

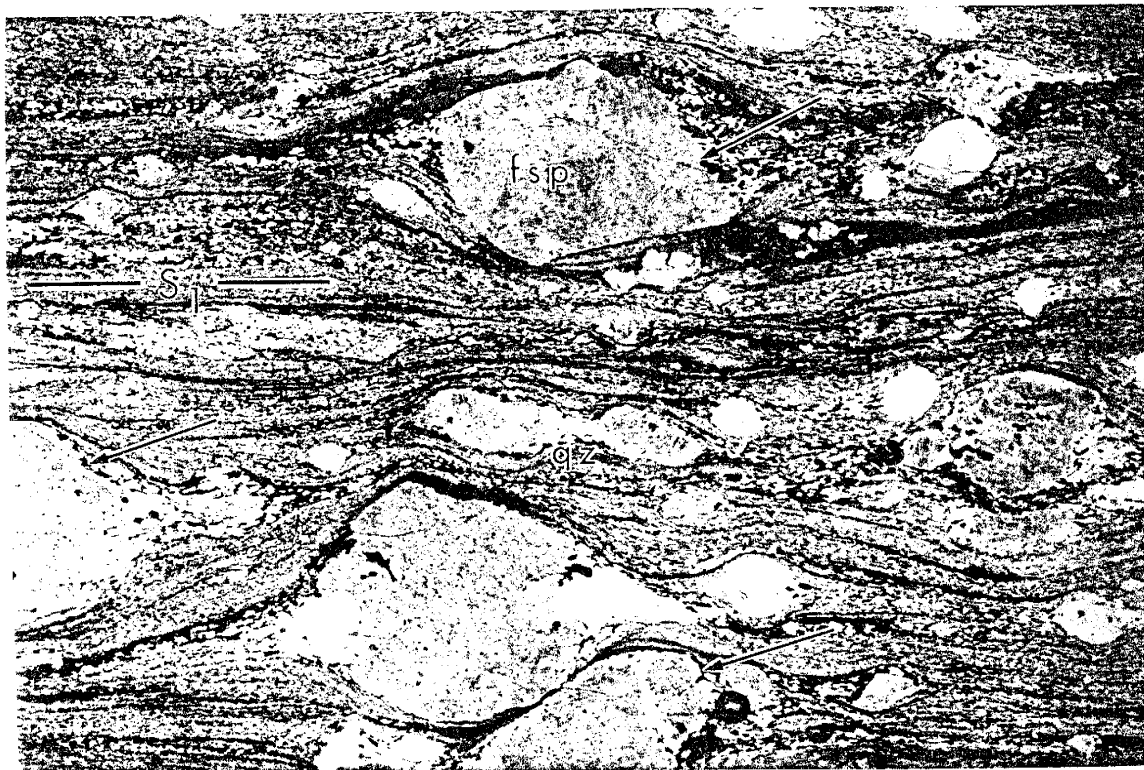


Figure 9: Photomicrograph of metavolcanic rock from southern portion of field area (sample 9171). View is perpendicular to S_1 and parallel to L_1 . S_1 is defined by felsic and mafic layers. Feldspar sigma porphyroblast system (fsp-top center) indicates sinistral and west-side-up motion. Feldspar porphyroblast in center of photo is boudinaged with quartz (qz) infilling neck between boudins. Arrows point to fractures in feldspar porphyroclasts. Plane-polarized light; 6mm across.

Kinematic Indicators

Kinematic indicators are seen on both the macroscopic and microscopic scale. Maximum asymmetry is visible in planes viewed perpendicular to foliation and parallel to lineation.

At the outcrop scale, sense-of-shear indicators include asymmetric folds within schists and quartzites and rare asymmetric pebble-foliation relationships in metaconglomerates. S-folds in cm-thick quartzite layers and a folded 3-cm-wide quartz vein in Workman Canyon exhibit west-up and sinistral motion. Disharmonic folds in cm-thick quartzite layers within schists south of Grandview Canyon are also asymmetrical, but indicate sinistral shear and west-side-down motion. Within metaconglomerate layers, elongate pebbles are generally symmetrical parallel to lineation, with rare asymmetric pebble-foliation relationships indicating sense-of-shear consistent with that found in folds and microstructures (Fig. 8d).

Within metavolcanic rocks, 0.5-2mm feldspar and quartz porphyroblast systems exhibit dominantly symmetrical tails. Asymmetrical structures are infrequently preserved in the form of quartz and feldspar sigma-type porphyroblast systems (cf. Passchier and Simpson, 1986) (Fig 9).. S-C fabrics (cf. Lister and Snoke, 1984) are preserved in quartzites and quartz-rich layers of deformed portions of the Strawberry Peak pluton (Fig. 11). C-surfaces are defined by mica-rich zones, and S-surfaces are defined by grain-shape preferred orientations of quartz and feldspar. The angle between S and C



Figure 10: Photomicrograph of pelitic schist from area between the Strawberry Peak and Capitol Peak plutons (sample 2141). View is perpendicular to S_1 and parallel to L_1 . Garnet (gt), biotite (bt), and andalusite (and) overgrow S_1 , while andalusite also defines L_1 . Plane-polarized light; 6mm across.

surfaces is generally between 40° and 45° with the exception of a sample from a shear zone within the Strawberry Peak pluton where S-C surfaces are nearly perpendicular. Regionally, porphyroclast systems and S-C fabrics indicate sinistral sense-of-shear with a dip-slip component, while locally, adjacent to and within the Strawberry Peak pluton, S-C fabrics record dextral and pluton-side-up motion.

In the northern portion of the study area, 0.7mm-2cm garnet porphyroblasts overgrow S_1 . Within 5 meters of the Strawberry Peak pluton Si/Se relationships in rare asymmetric porphyroblast systems indicate pluton-side-up and dextral motion along the SW contact and pluton-side-up (L_1 is down dip) along the NW contact. (Fig. 12). Garnet porphyroblasts distal to the pluton are locally fractured and exhibit no apparent asymmetry (Fig. 10). Shear bands consistent with sinistral motion are present in a garnet-mica schist containing fractured garnets north of Ash Canyon.

Sense-of-shear indicators throughout the study area generally record sinistral strike-slip motion with a dip-slip component (Fig. 7). Exceptions exist in zones adjacent to, and within, the Strawberry Peak pluton. Sense-of-shear indicators within 10 m of the contact consistently indicate pluton-side-up. Dextral motion along the SW contact is a result of pluton-side-up motion and the transition of L_1 from SE to NE plunging. Petrographic analysis of thin sections from discrete shear zones within the Strawberry Peak pluton yielded inconsistent results. Shear zones in the southern part of the pluton record



Figure 11: Photomicrograph of granite mylonite from internal shear zone, Strawberry Peak pluton (sample 4142). View is perpendicular to S_1 and parallel to L_1 . S-C fabric indicates top to the right motion which translates into sinistral and east-side up motion in real coordinates. S-surfaces are defined by quartz ribbons. C-surfaces defined by biotite parallel the macroscopic foliation (S_1). Crossed polars; 3mm across.

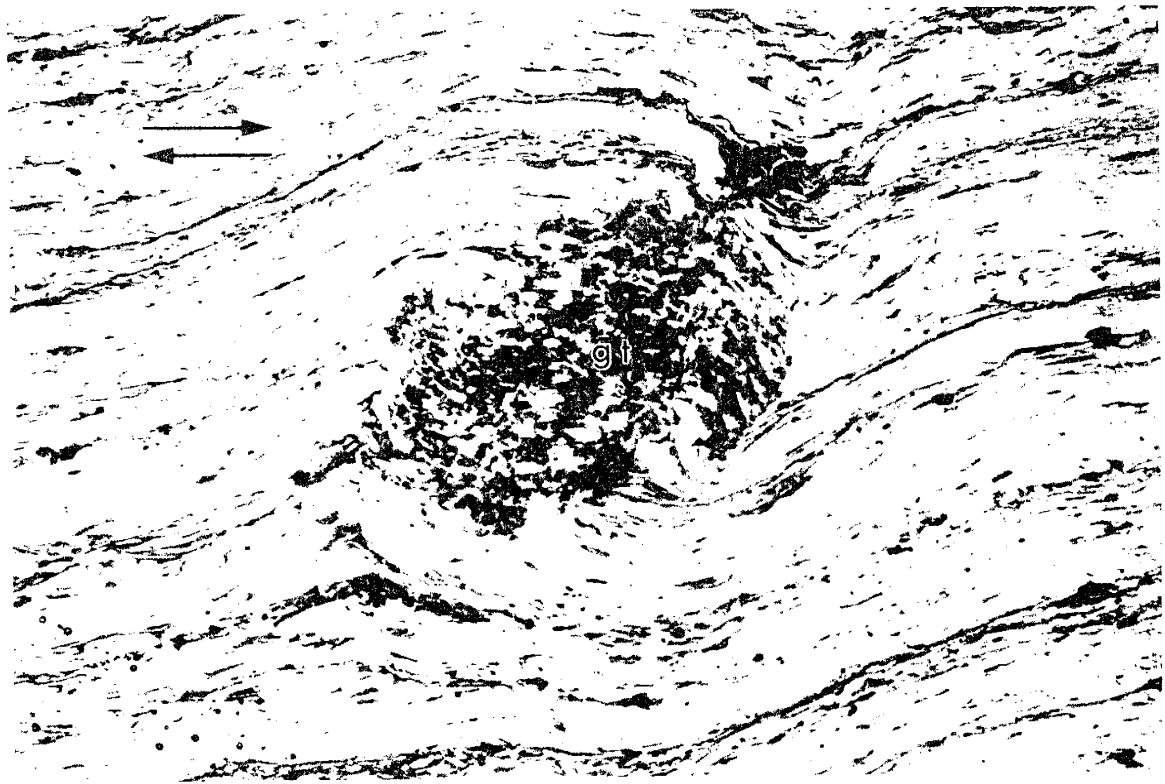


Figure 12: Photomicrograph of pelitic schist located within 5 meters of the SW contact with the Strawberry Peak pluton (sample 41416). View is perpendicular to S_1 and parallel to L_1 . Garnet porphyroblast overgrows S_1 with minor rotation. Sense of shear indicates pluton-side up motion. Plane-polarized light; 6mm across.

dextral motion whereas those from the northeast portion record sinistral motion. These differences are possibly related to tightening of the fold during intrusion.

Plutonic Rocks: Structure and Contact Relationships

Three felsic intrusive bodies are present within the study area, each exhibiting distinctive structural characteristics. The previously unmapped Boki granite, located along the eastern margin of the study area, is strongly deformed. This intrusive body is characterized by a well-developed tectonic foliation and a well-developed mineral lineation defined by elongate K-feldspar and plagioclase grains. The orientations of S_1 and L_1 within the Boki granite is parallel to, and continuous with, those found in adjacent supracrustal rocks. Contacts vary from concordant in the north to highly discordant in the south, with respect to S_1 .

The Strawberry Peak granite is variably deformed, exhibiting a well-developed tectonic foliation within 10 m of contacts with supracrustal rocks and in a number of discrete shear zones. The bulk of the pluton is weakly to undeformed. The NW contact strikes approximately N45E and is parallel to S_1 and S_0 . Small scale variations in orientation of the contact are mirrored by variations in orientation of S_1 . Within the pluton, within 3-5 m of the contact, S_1 is well developed; however, S_1 is generally nonexistent at distances beyond 10 m into the pluton. Meter scale xenoliths of country rock are restricted to the deformed margin of the pluton, and S_1 passes unobstructed

through them. Similar relationships are observed along the E and SW margins of the pluton where the contacts strike N-S and NW respectively (Figs. 4 and 6).

Shear zones within the Strawberry Peak granite are generally 5-10 m wide with a strong planar fabric in the center which dissipates toward the margins. In the southern portion of the pluton, shear zones strike generally N-S. A NE-striking zone of high shear strain which snakes through the central portion of the pluton, where it anastomoses around, and is concentrated along, contacts with 10-20-m-long pods of a finer-grained, plagioclase-rich phase that is intrusive into the main stock. These intrusive pods show no evidence of deformation.

The dominant fabric in the Capitol Peak quartz monzonite is a magmatic foliation defined by 1-4 cm euhedral plagioclase and K-feldspar phenocrysts and coherent cm-size books of biotite. Quartz crystals are equant, ranging from 1 to 5mm in diameter. The orientation of this foliation is approximately ENE with shallow dips to the SSE (Fig. 6). Within the pluton, within 3-5 m of the contact with supracrustal rocks, this magmatic foliation is overprinted by a well-developed tectonic foliation. Feldspars and quartz are elliptical with axial ratios up to 4:1 in a 1 m wide band adjacent to supracrustal rocks. Over the next several meters axial ratios fall to approximately 2:1 and feldspars are subrounded. The tectonic fabric is steepest within several centimeters of the contact, becoming more shallow with distance from the contact with supracrustal rocks. The orientation of the tectonic fabric within 1

m of the contact is quite variable, running parallel to the irregular margin of the contact. Veins within the country rocks are variably deformed as well. The dominant regional foliation (S_1) passes through early veins, which are in turn crosscut by late, unfoliated veins. Rare xenoliths within the Capitol Peak pluton exhibit foliation orientations that are discordant to those found in the adjacent supracrustal rocks.

A large block of quartzite in the area south of Workman Canyon is bounded by brittle structures and orientations of S_1 within this block do not coincide with the regional trends (Fig. 4, and Fig. 5, section A-A'). The presence of coarse-grained quartz, muscovite, K-feldspar, and xenoliths of foliated country rock in several m-wide fracture zones (Fig. 8e), coupled with proximity to the Capitol Peak pluton indicate this area of quartzite may be shallowly underlain by the Capitol Peak pluton.

Metamorphism

Metamorphic Grade

Evaluation of mineral assemblages, microprobe data, and microstructures reveal spatial variations in metamorphic grade. The southern area, south of Grandview Canyon will be described first, followed by a description of the northern portion of the field area. A third section will provide descriptions of areas adjacent to intrusive bodies.

While factors such as water content and strain rate can affect deformation mechanisms active in minerals undergoing deformation,

detailed petrographic examination of microstructures can provide insight regarding temperature of deformation (c.f. Bouillier and Bouchez, 1978; Simpson, 1985). In general, at greenschist facies conditions, feldspar tends to deform by brittle fracturing, and individual grains commonly exhibit undulose extinction and deformation twinning. This is in contrast to deformation of feldspar at amphibolite facies conditions where feldspar deforms by ductile processes and commonly shows evidence for dynamic recrystallization. Quartz will behave ductilely throughout greenschist and amphibolite grade conditions, although quartz ribbons are generally monocrystalline at greenschist facies conditions and exhibit a granoblastic polygonal texture at amphibolite facies conditions.

Southern area

Mineral assemblages from the southern portion of the study area indicative of metamorphic grade include quartz - K-feldspar - albite - epidote - chlorite \pm biotite \pm muscovite in felsic metavolcanic rocks, and (Ferro) hornblende - plagioclase - chlorite - epidote - sphene in amphibolites. Syntectonic chlorite and epidote in metavolcanic rocks and the occurrence of syntectonic chlorite and sphene in amphibolites indicate deformation occurred below 550°C (cf. Liou et al., 1974).

Further constraints on the maximum temperature of metamorphism come from microprobe analysis of feldspar from a metavolcanic rock (sample 9176) north of Treasure Mountain. Microprobe analysis was conducted at

New Mexico Tech using a Cameca SX-100 electron microprobe. Quantitative wavelength-dispersive geochemical analysis with a 20.0 nA beam at 15.0 kV was conducted on several individual feldspar grains to determine Ca content. The beam was broadened to 10 μ m for Na analysis to avoid Na loss. Qualitative backscatter electron imaging was used to locate feldspar grains, and the entire section was scanned using x-ray mapping to determine if Ca was present in feldspars. Although both twinned and untwinned feldspar are present, this analysis showed that both phases are nearly pure albite (Table 1). The work of Liou et al. (1974) indicates An content will increase dramatically above 475 $^{\circ}$ C.

Microprobe analysis of amphibole from dark-green amphibolite (sample HC-5, Fig. 5) in Hembrillo Canyon reveals hornblende with moderate Al content (Table 2). Experimental work by Spear (1981) suggests that the reaction hornblende + plagioclase + quartz = actinolite + chlorite + epidote + albite + quartz will go to completion below 475 $^{\circ}$ C.

Microstructural evidence of metamorphic grade includes quartz ribbons with subgrain formation and sweeping undulose extinction. Feldspars are characterized by abundant deformation twins. Metavolcanic rocks in Hembrillo Canyon are characterized by core and mantle structures in feldspar and quartz porphyroclasts and extensive subgrain formation in 1-3mm quartz lenses. Feldspar porphyroclasts are commonly fractured and extended with recrystallized grains along microcracks and necks between boudins (Fig. 9). Felsic grains exhibit dominantly sutured to lobate grain

Feldspar Analysis			
Oxide	Feldspar 1	Feldspar 2	Feldspar 3
	Wt. %	Wt. %	Wt. %
SiO ₂	67.67	67.25	66.97
Al ₂ O ₃	20.09	20.08	19.88
CaO	0.25	0.28	0.3
FeO	0.05	0.1	0.08
Na ₂ O	11.71	11.31	11.25
K ₂ O	0.07	0.1	0.11
Total	99.83	99.12	98.6
An content	1.15	1.36	1.45

Table 1: Oxide weight percent of feldspars from microprobe analysis of metavolcanic rock. Data indicate feldspars are nearly pure albite.

Oxide	Ferro Hornblende	Tschermakitic Hornblende
	Wt. % ($\pm 1\sigma$)	Wt. % ($\pm 1\sigma$)
Na ₂ O	0.81 \pm 0.27	1.41 \pm 0.17
MgO	8.36 \pm 1.62	10.1 \pm 0.84
Al ₂ O ₃	5.72 \pm 1.30	13.2 \pm 1.5
SiO ₂	47.4 \pm 2.27	44.2 \pm 1.3
Cl	0.37 \pm 0.28	0.31 \pm 0.05
K ₂ O	0.57 \pm 0.31	0.43 \pm 0.04
CaO	10.9 \pm 0.70	11.9 \pm 0.17
TiO ₂	0.76 \pm 0.56	0.50 \pm 0.14
MnO	0.58 \pm 0.12	0.42 \pm 0.03
FeO	23.6 \pm 2.02	17.0 \pm 0.66
Total	99.1	99.49
	n=17	n=25

Table 2: Average oxide weight percent of amphibole from microprobe analyses of amphibolite. Data indicate two distinct amphibole phases. Ferro hornblende from amphibole in Hembrillo Canyon (sample hc-5) exhibits significantly lower Al and Na content, and higher Si content than Tschermakitic hornblende from amphibolite adjacent to Strawberry Peak pluton (sample 1084).

boundaries, strong undulose extinction, and variable grain size (Fig. 13a). Dynamic recrystallization of quartz is indicated by the presence of undulose extinction and abundant subgrain and new grain formation (cf. Passchier and Trouw, 1996).

Northern area

Within pelitic schists north of Strawberry Peak, the typical mineral assemblage is muscovite - quartz - biotite - garnet - andalusite \pm staurolite. Andalusite and biotite are present in two distinct phases, one defining a lineation (L_1) in the plane of S_1 , and a second overgrowing S_1 (Fig. 10). Rare grains of staurolite and abundant garnet consistently overgrow S_1 .

Microstructures from the northern area differ from those in the southern area. Feldspar and quartz generally occur in a polygonal mosaic with straight to curved grain boundaries. Metasedimentary rocks dominated by quartz and feldspar display a uniform grain size (Fig. 13b). Fractured and extended feldspar is not observed and polycrystalline quartz ribbons display a granoblastic polygonal texture with weak to nonexistent undulose extinction.

Contact Metamorphism

Rocks adjacent to both the Strawberry Peak and Capitol Peak plutons record evidence of contact metamorphism. Evidence for contact metamorphism adjacent to the Strawberry Peak pluton includes microprobe

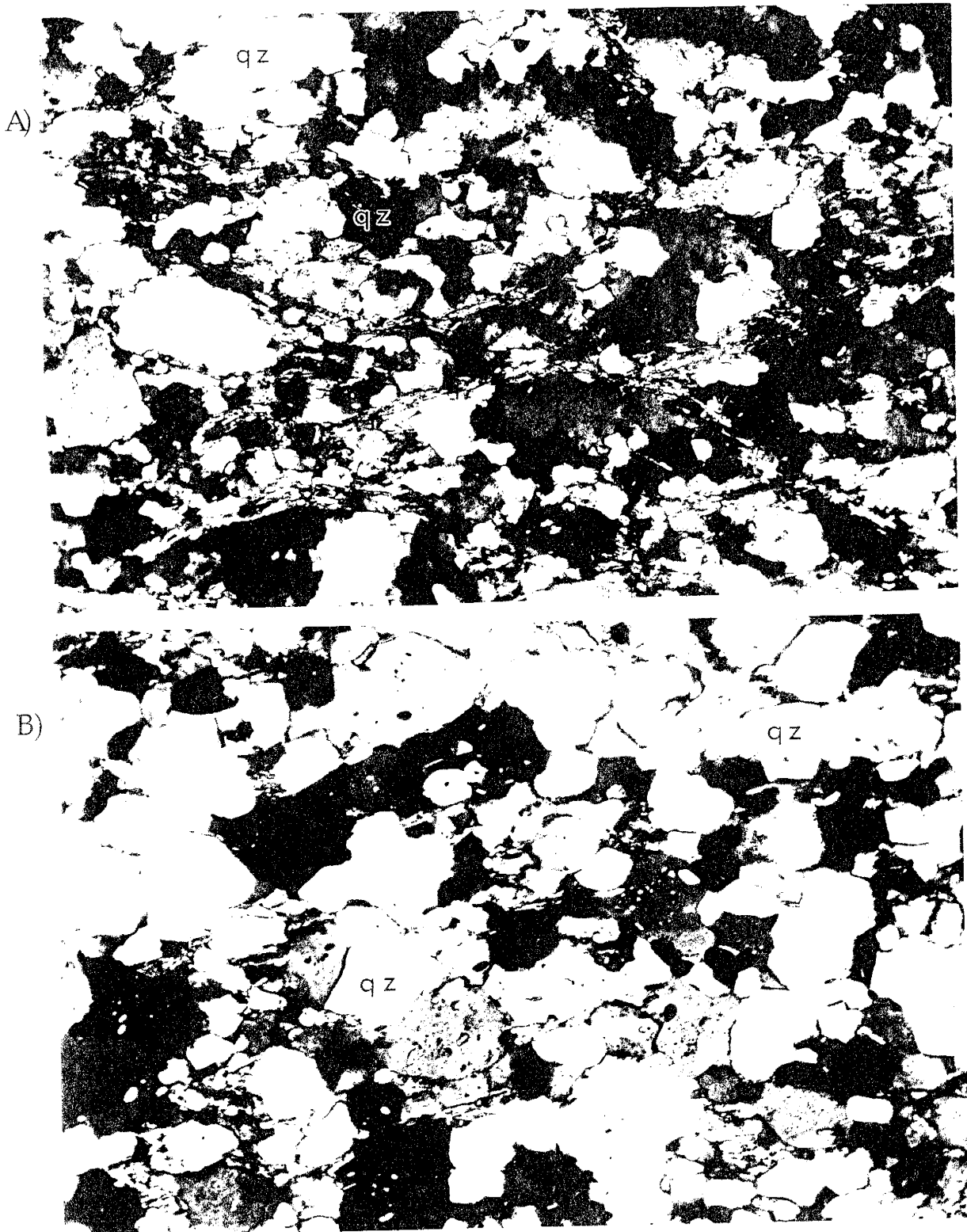


Figure 13: Photomicrographs showing variations in quartz microstructures. In both photos view is perpendicular to S_1 and parallel to L_1 . Crossed polars; 3mm across. (A) Quartzofeldspathic schist from the southern portion of the field area (sample hc-8). Quartz grains exhibit sutured grain boundaries, moderate to strong undulose extinction, and variable grain size. (B) Quartzofeldspathic schist from northern portion of field area (sample 10217). Quartz grains are relatively uniform in size, exhibit moderate to strong undulose extinction, and relatively uniform grain size.

data, microstructural evidence, and metamorphic mineral growth, whereas evidence adjacent to the Capitol Peak pluton is limited to microstructures and metamorphic mineral growth. Microprobe analysis of amphibole from an amphibolite adjacent to the southernmost outcrop of the Strawberry Peak pluton reveals compositions consistent with middle to upper amphibolite facies metamorphic conditions (Table 2), (Spear, 1981). Al and Na contents show a marked increase and Si content decreases with respect to amphibole distal to the pluton.

Microstructures in the same amphibolite, that are characteristic of contact metamorphism, include straight grain boundaries in feldspar with a lack of undulose extinction, and a moderately developed granoblastic polygonal fabric (Fig. 14). A well-developed foliation defined by slightly elongate, strain-free hornblende and plagioclase is parallel to, and continuous with the regional tectonic foliation.

The absence of sphene within amphibolite adjacent to the Strawberry Peak pluton is also indicative of middle to upper amphibolite facies conditions if one assumes the protolith for this amphibolite is similar to other amphibolites in the study area which contain abundant syntectonic sphene (Spear, 1981). Pelitic schists NW and SW of the Strawberry Peak pluton contain abundant 0.5 - 1 mm garnets. With proximity to the Strawberry Peak pluton, the frequency of garnet decreases and individual garnet porphyroblasts increase notably in size. Within 20 m of the contact garnets average 1-3 cm in diameter and overgrow the tectonic foliation.

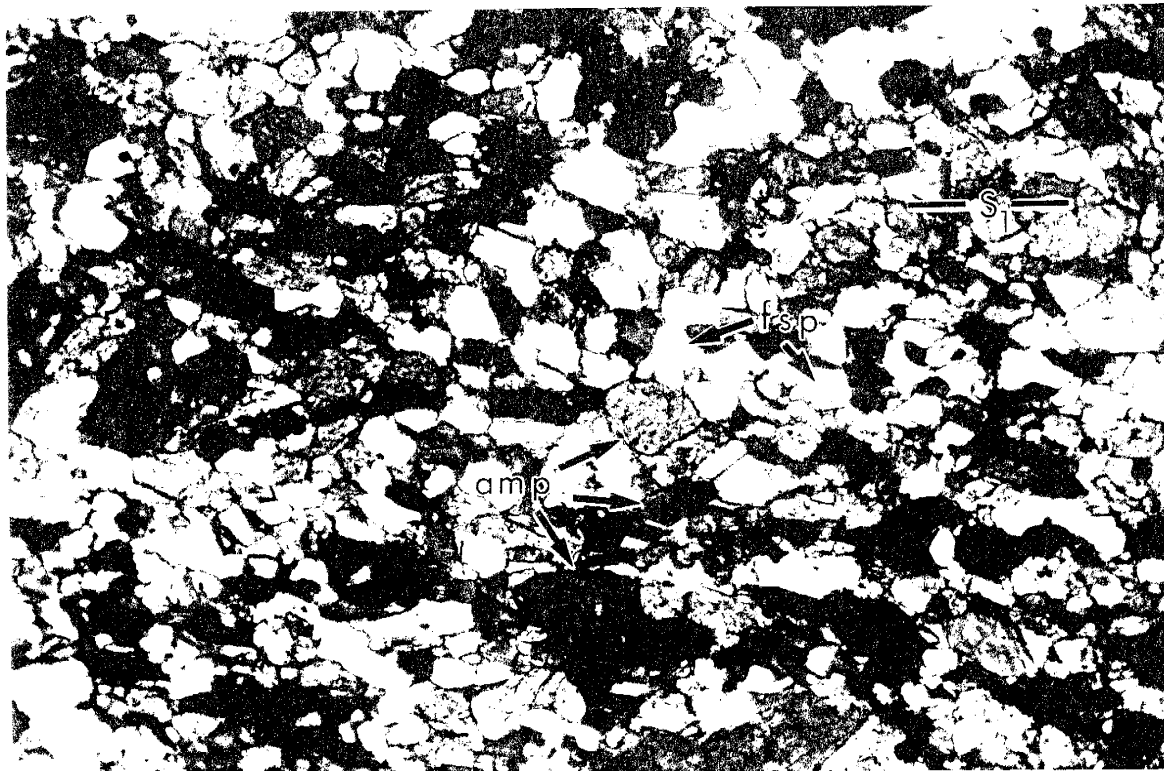


Figure 14: Photomicrograph of amphibolite adjacent to the Strawberry Peak pluton (sample 1084). View is perpendicular to S_1 and parallel to L_1 . Feldspar and amphibole (amp) grains exhibit straight grain boundaries and a lack of undulose extinction with a well-developed granoblastic polygonal texture. Crossed polars; 6mm across.

In the area between the Strawberry Peak pluton and Capitol Peak pluton post-tectonic andalusite and staurolite occur. The existence of these minerals is restricted to pelitic schists and is equidistant from the two intrusive bodies. As a result, it is unclear whether growth is related to intrusion of one or the other, or perhaps both of the plutons.

Within meta-arkose located 1 m from the contact with the Capitol Peak pluton, feldspar and quartz exhibit a well developed granoblastic polygonal fabric. Evidence for grain boundary migration (bulging) and undulose extinction are common, although grain boundaries are dominantly straight to curved.

Thermochronology

Both U/Pb and $^{40}\text{Ar}/^{39}\text{Ar}$ dating techniques have been applied to Proterozoic rocks for this study. Both techniques date the time at which some mineral cools through a specific temperature. This temperature, at which the isotopic system is closed to diffusion, is referred to as the "closure temperature". In the case of U/Pb dating, igneous zircon cools through the closure temperature at approximately the time of crystallization. Due to the high closure temperature of zircon ($\sim 750^\circ$) (Ghent et al., 1988), the isotopic system is generally unaffected by subsequent heating events. $^{40}\text{Ar}/^{39}\text{Ar}$ thermochronology dates the time at which metamorphic minerals cool through the temperature at which Ar diffusion ceases. As a result of the

relatively low closure temperatures of metamorphic minerals with respect to Ar (amphibole 500° - 550° C, Harrison, 1981; muscovite 350° - 400° C, Hames and Bowring, 1994; biotite 300° - 350° C, Harrison et al., 1985), subsequent heating events may more easily reset the isotopic system.

Igneous zircon from a metavolcanic rock (Fig. 4, sample 9176) from the southern portion of the field area and from the Strawberry Peak pluton (Fig. 4, sample 3151) were prepared at the University of Wyoming for U/Pb analysis. Preliminary results indicate magmatic ages of ~1650 Ma for the metavolcanic, and ~1630 Ma for the Strawberry Peak pluton (K. Chamberlain, written comm., 1997). In both samples the grains are euhedral, and multiple morphologies or inherited cores are absent. Thus it seems unlikely that these grains are inherited or detrital, and the ages are interpreted to represent timing of crystallization of the respective units.

Six samples were prepared for $^{40}\text{Ar}/^{39}\text{Ar}$ analysis at the New Mexico Geochronology Research Laboratory. The samples were taken from a deformed vein associated with the Capitol Peak pluton (sample 10217 muscovite), a pelitic schist in the northern portion of the study area (sample 2141 biotite), a shear zone within the Strawberry Peak pluton (sample 4145 muscovite), an amphibolite adjacent to the Strawberry Peak pluton (sample 1084 amphibole), and an amphibolite in the southern portion of the field area (sample 3103 biotite and amphibole) (Fig. 4). Of these samples, three yielded concordant plateau ages (10217 muscovite, 4145 muscovite, and 3103 biotite),

while age spectra of the other three samples exhibit varying degrees of complexity.

Muscovite age spectra obtained from the Strawberry Peak pluton (sample 4145) and Capitol Peak pluton (sample 10217) yield plateau ages of 1454.5 ± 1.9 Ma and 1438.4 ± 0.9 Ma, respectively (Fig. 15a and b). Sample 4145 reveals some discordance for the first 5% of the age spectrum, whereas sample 10217 has a flat age spectrum for greater than 95% of the ^{39}Ar released. $^{40}\text{Ar}/^{39}\text{Ar}$ analysis of foliation-forming biotite from sample 3103 yields a well defined plateau age of 1400 ± 2 Ma (Fig. 15c). This sample shows some discordance in the first and last 5% of the ^{39}Ar released.

The remaining three $^{40}\text{Ar}/^{39}\text{Ar}$ analyses yield somewhat more discordant age spectra (Figs. 15d and 16). Analysis of biotite grains from a pelitic schist located in the area between the Strawberry Peak and Capitol Peak plutons (sample 2141) reveals ages between 1400 and 1420 Ma for approximately 65% of the ^{39}Ar released (Fig. 15d). The grains analyzed were relatively large (1-2mm) and overgrow the main foliation (S1). Younger and older age steps are possibly related to the inclusion of other phases.

Analysis of amphibole from a black amphibolite adjacent to the southernmost outcrop of the Strawberry Peak pluton (sample 1084) and from a green amphibolite (sample 3103) in the southern portion of the field area show rather complex age spectra as well. Sample 1084 exhibits variable K/Ca ratios for the first half of the age spectrum and corresponding variability in

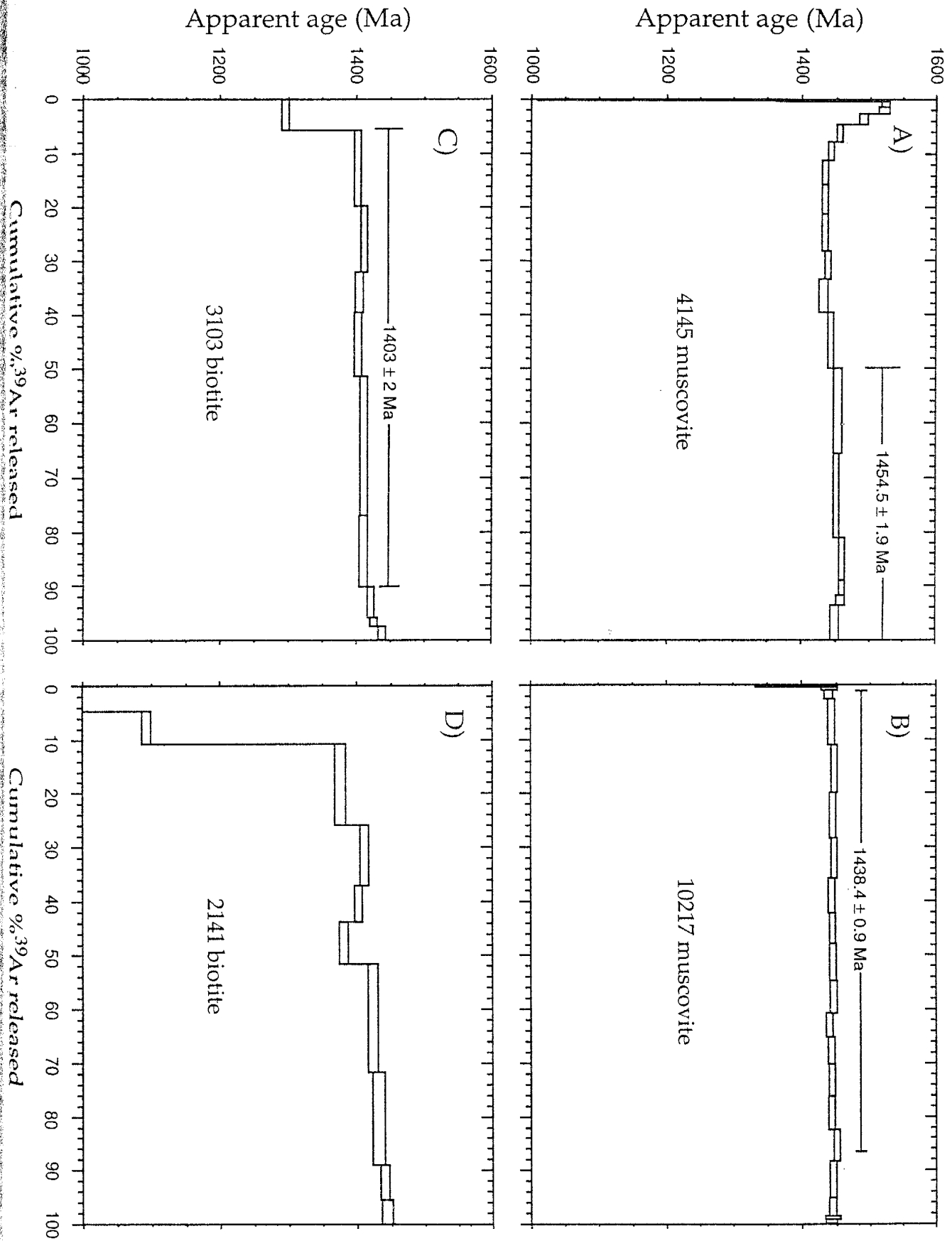


Figure 15: $^{40}\text{Ar}/^{39}\text{Ar}$ age spectra for muscovite and biotite. Plateau ages are shown on figures A, B, and C. Sample locations are shown on figure 5.

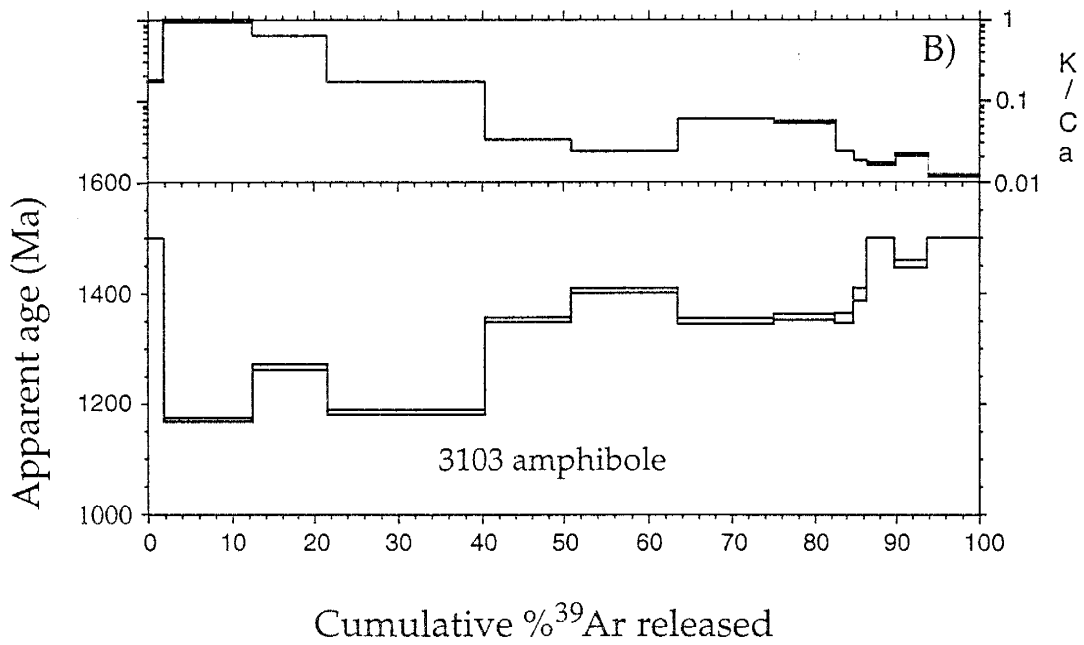
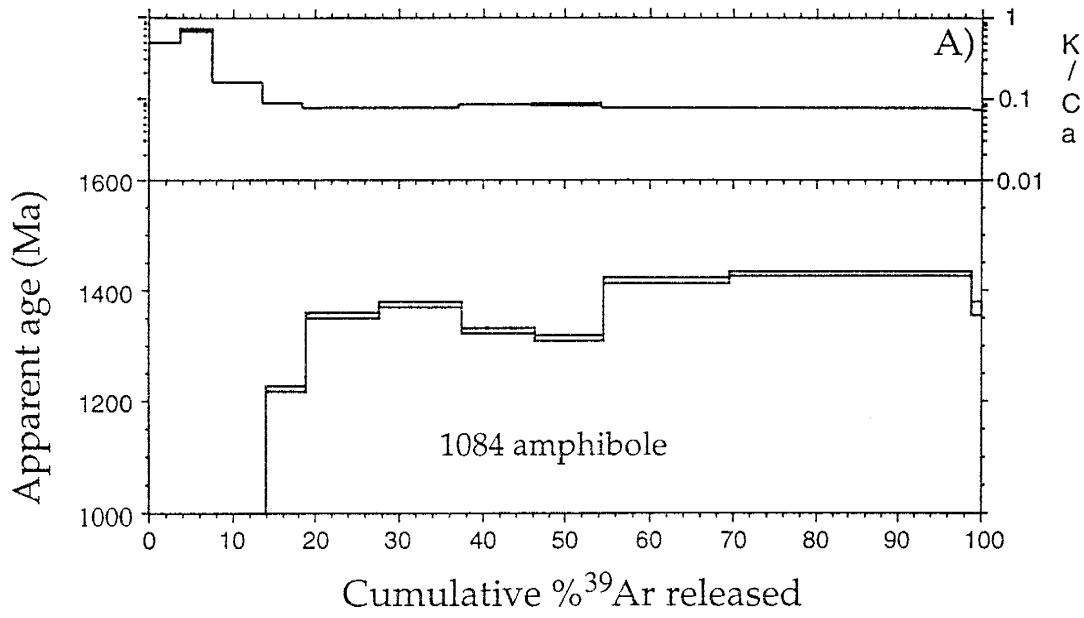


Figure 14: $^{40}\text{Ar}/^{39}\text{Ar}$ age spectra for amphibole. Discordance in age spectrum are coincident with variations in K/Ca ratios. Sample locations are shown in figure 5. Microprobe data is shown in table 2.

apparent ages (Fig. 16a). The second half of the age spectrum shows relatively flat K/Ca ratios and the corresponding apparent age is relatively flat at ~1420 Ma. Amphibole from sample 3103 yields a highly discordant age spectrum which corresponds to variable K/Ca ratios (Fig. 16b). Variations in K/Ca ratios, and corresponding variations in the age spectra is possibly related to inclusions of a fine-grained phase with K/Ca ratios different from those of the host amphibole.

Discussion

Deformation

Mid-crustal deformation during the Proterozoic resulted in folding of bedding (S_0) into a map scale syncline and development of a penetrative axial planar cleavage (S_1) in the San Andres Mountains of south-central New Mexico. Sense of shear within supracrustal rocks, viewed parallel to L_1 and perpendicular to S_1 , is dominantly sinistral strike-slip with a dip-slip component. Due to the doubly plunging nature of the syncline and the associated stretching lineation, it is unclear whether east-up or west-up motion was active. Folding of S_0 and formation of symmetrical fabrics is likely related to a component of coaxial deformation, whereas asymmetrical structures recording sinistral strike-slip motion are consistent with a component of noncoaxial shear.

S_1 and the syncline are folded about an E-trending, steeply E-plunging fold axis centered on the late-syntectonic Strawberry Peak pluton. If folding of

the syncline, S_1 , and L_1 were related to N-S shortening after development of these structures, we would expect to see a progressive change in orientation of L_1 from NE-plunging in the north to horizontal in the vicinity of the Strawberry Peak pluton, then SE-plunging in the south. Instead, with proximity to the Strawberry Peak pluton, L_1 tends to steepen, becoming subparallel to the E-W fold axis. This indicates that folding about an E-W axis, and the resulting doubly plunging nature of the syncline is temporally related to intrusion of the Strawberry Peak pluton.

Metamorphism

South of Grandview Canyon mineral assemblages, microstructures, and microprobe data indicate deformation at slightly lower grade conditions than those in the north. The mineral assemblage (ferro)hornblende - plagioclase - chlorite - epidote - sphene in amphibolites south of Grandview Canyon, coupled with the presence of nearly pure albite in metavolcanic rocks, is consistent with deformation at approximately 475° C (Liou et al., 1974; Spear, 1981). Microstructures in felsic grains from the southern area including variable grain size, sutured to lobate grain boundaries with subgrain formation, strong undulose extinction, and deformation twinning in feldspars are indicative of middle to upper greenschist facies conditions (Simpson, 1985; Passchier and Trouw, 1996). Within metavolcanic rocks, feldspar porphyroclasts are fractured with recrystallized grains along microcracks, also an indication of middle to upper greenschist facies conditions (Simpson, 1985). South of Grandview Canyon the tectonic

foliation is not overgrown by metamorphic minerals, indicating that deformation was coincident with metamorphism.

Mineral assemblages and microstructures in the northern area indicate slightly higher grade conditions. The assemblage muscovite - quartz - biotite - garnet - andalusite \pm staurolite indicates temperatures above 500° C with pressures between 2 and 4 kb based on the petrogenetic grid of Yardley (1989). This is consistent with amphibolite facies microstructures such as straight to curved grain boundaries, a moderately developed granoblastic polygonal texture, and weak to nonexistent undulose extinction (Simpson, 1985). In the northern area, the tectonic foliation is overgrown by staurolite, andalusite, and biotite indicating that metamorphism outlasted deformation.

Constraints on the timing of deformation and metamorphism provided by igneous history

Distinction between pre-, syn-, and post-tectonic intrusions can be problematic and a number of different criteria must be evaluated. Paterson and Tobisch (1988) outline the most critical of these factors: 1) determination of whether foliations in the pluton are tectonic or magmatic; 2) patterns of foliations in and around the pluton; 3) correlation of foliations in the pluton with those in the surrounding rock; and 4) examination of cleavage-porphyroblast relations in the surrounding rock. Examination of criteria in the central San Andres Mountains helps determine the relative timing of deformation, metamorphism, and intrusion.

The Boki pluton is strongly deformed with a penetrative tectonic foliation that is parallel to, and continuous with, the regional tectonic foliation. This is especially evident where the foliation is at high angles to pluton-country rock contacts. No evidence for contact metamorphism is evident within the wall rocks. These characteristics are consistent with pre-tectonic plutonism, although early syntectonic emplacement is possible (cf. Paterson et al., 1989).

Deformation associated with the Strawberry Peak pluton is restricted to the margins of the pluton and several discrete shear zones within the pluton. Adjacent to the pluton the foliation tends to mirror variations in orientation of the contact. Evidence for contact effects include an increase in garnet porphyroblast size overgrowing the regional tectonic foliation with proximity to the pluton, microprobe data indicating growth of higher temperature foliation-defining amphibole adjacent to the pluton, and the occurrence of higher temperature microstructures with proximity to the pluton. The overall shape of the Strawberry Peak pluton is generally concordant with the regional structure. These characteristics are consistent with syntectonic emplacement as outlined by Paterson and Tobisch (1988, and references therein) and Paterson et al. (1989).

The Capitol Peak pluton shares several characteristics of syntectonic emplacement with the Strawberry Peak pluton including the orientation of foliations and higher temperature microstructures proximal to contacts. A well-developed magmatic foliation subparallel to the tectonic foliation within

wall rocks is also suggestive of late-syntectonic emplacement (Paterson et al., 1989). The occurrence of early, foliated veins crosscut by late, unfoliated veins indicate that late phases of intrusion post-date deformation.

Variations in the timing and character of deformation and metamorphism from north to south can be explained by late-syntectonic intrusion in the north and the absence of plutonic rocks to the south. Increased thermal gradients related to intrusion of the Strawberry Peak and Capitol Peak plutons resulted in higher temperature microstructures and post-kinematic mineral growth in the area between these two plutons. The absence of post-kinematic mineral growth and lower temperature microstructures distal to the plutons supports the interpretation that deformation was coincident with metamorphism regionally, while locally, adjacent to intrusive bodies, metamorphism outlasted deformation.

Thermochronology and Regional Implications

Crystallization ages of ~1650 Ma for deformed metavolcanic rocks and ~1630 Ma for the late-syntectonic Strawberry Peak pluton provide constraints on the maximum and minimum ages of deformation. The timing of this deformation event is similar to that proposed for Proterozoic rocks found in the transition zone of Arizona (e. g., Karlstrom and Bowring, 1990) and the Magdalena Mountains of central New Mexico (Bauer and Williams, 1994).

$^{40}\text{Ar}/^{39}\text{Ar}$ ages from the San Andres Mountains range from ~1400 Ma to ~1450 Ma. This suggests that a reheating event occurred at temperatures at,

or in excess of, the closure temperature for amphibole ($\sim 500^{\circ}\text{C}$). A lack of microstructures associated with annealing indicate that these temperatures were short lived. Although an absolute age of emplacement of the Capitol Peak pluton is not available, field evidence indicates that it is similar in age to the Strawberry Peak pluton.

Data from the San Andres Mountains support tectonic models that call for major deformation in the southwest at ~ 1650 Ma during the Mazatzal Orogeny, and a subsequent thermal event at ~ 1450 . Evidence for ~ 1400 Ma deformation in central and northern New Mexico comes from areas that have been affected by multiple deformation events. Proterozoic rocks in the San Andres Mountains show evidence for one progressive deformational event. Other Proterozoic exposures in New Mexico that are characterized by D_1 fabrics include the Magdalena Mountains (Bauer and Williams, 1994) and portions of the Ladrone Mountains (Pollock, 1994). Thus it appears that effects of ca. 1400 deformation are confined to other portions of the state, possibly as a result of heterogeneous strain, and the San Andres Mountains of south-central New Mexico provide an unobstructed view of ca. 1650 Ma deformation in southwest North America.

While the timing of this event indicates the deformation is likely associated with a D_1 event, the possibility exists that deformation in the San Andres Mountains represents a D_2 event. Comparison of structural and metamorphic trends in central New Mexico (table 3) suggests that D_1 deformation in the San Andres Mountains is similar in style to D_2

Event	Worker / Area	Marcoline, Manzano Mountains	Thompson et al., Manzano Mountains	Pollack, Ladron Mountains	Bauer and Lozinsky, Caballo Mountains	Bauer and Williams, Magdalena Mountains
D1)	Geometry	unknown	NE-Striking	WNW-striking	E-striking	N- to NE striking
	Kinematics	unknown	ductile extension	Dextral strike- slip	dextral strike- slip	unknown
	Timing	unknown	1.44 Ga	unknown (likely 1.6 Ga)	unknown (likely 1.6 Ga)	1.66 Ga
D2)	Geometry	NNE-striking Isoclinal to open folds	NE-striking	NE-striking tight to isoclinal folds	E-striking tight upright folds	not observed
	Kinematics	East-up shear	East-up shear	East-down shear	unknown	not observed
	Timing	1.4 Ga	1.35 Ga	unknown	unknown	not observed

Table 3: Brief summary of Proterozoic deformational events from central New Mexico. Data from Bauer and Lozinsky (1986), Thompson et al. (1991), and Bauer and Williams (1994), Pollock (1994), Marcoline (1996),.

deformation in the Caballo and Manzano Mountains in that it produced upright, tight to isoclinal folds at moderate metamorphic grades. Conversely, kinematics are more similar to D_1 events in the Ladrone and Caballo Mountains in that the dominant motion is strike-slip. The orientation of the dominant fabric in the San Andres Mountains is at a high angle to D_1 fabrics in the Ladrone and Caballo Mountains, and subparallel to D_1 fabrics in the Magdalena Mountains. In light of these conflicting pieces of evidence, the possibility exists that deformation in the San Andres Mountains is associated with a D_2 event. If this is the case, then all evidence for D_1 deformation has been erased, and the D_1 and D_2 events must have occurred within a relatively short time frame (i.e. two deformation events between 1650 Ma and 1630 Ma).

Conclusion

Proterozoic rocks of the San Andres Mountains preserve evidence for one progressive penetrative deformational event in contrast to many other areas of New Mexico which show evidence for at least two deformational events. Microstructures, mineral assemblages, and microprobe data indicate deformation occurred at middle to upper greenschist facies conditions in the south and upper greenschist to amphibolite facies conditions in the north. Higher grade conditions in the north are related to syn-tectonic intrusion of the Strawberry Peak and Capitol Peak plutons. The timing of this progressive deformational and metamorphic event is coincident with the Mazatzal orogeny at 1650 Ma. Deformation was followed by a reheating event at 1400

Ma that reset Ar isotopic systems, yet apparently left no evidence of metamorphism and deformation. The 1400 Ma heating event correlates with widespread plutonism, metamorphism, and deformation proposed for northern and central New Mexico by several recent workers (Thompson et al., 1991; Grambling and Dallmeyer, 1993; and Marcoline et al., 1996). It is proposed that D_1 , as described in the San Andres Mountains, correlates with the 1.6 Ga D_1 in other areas of New Mexico, many of which have been overprinted by 1.4 Ga deformation that was not recorded in the San Andres Mountains.

REFERENCES

- Alford, D. E., 1987. Geology and geochemistry of the Hembrillo Canyon Succession, San Andres, Sierra, and Dona Ana Counties, New Mexico. M. S. Thesis, New Mexico Institute of Mining and Technology, Socorro, 180 p.
- Bauer, P. W., 1993. Proterozoic tectonic evolution of the Picuris Mountains, northern New Mexico. *The Journal of Geology*, v 101, p 483-500.
- Bauer, P. W., and Williams, M. L., 1985. Structural relationships and mylonites in Proterozoic rocks of the northern Pedernal Hills, central New Mexico, in ed., *New Mexico Geologic Society Guidebook, 36th Field Conference*, p. 141-145.
- Bauer, P. W., and Lozinsky, R. P., 1986. Proterozoic geology of supracrustal and granitic rocks in the Caballo Mountains, southern New Mexico. *New Mexico Geologic Society Guidebook, 37th Field Conference*, p. 143-149.

- Bauer, P. W., and Williams, M. L., 1989. Stratigraphic nomenclature of Proterozoic rocks, northern New Mexico: revisions, redefinitions, and formalization. *New Mexico Geology*, v. 11, no. 3, p. 45-52.
- Bauer, P. W., Karlstrom, K. E., Bowring, S. A., Smith, A. G., and Goodwin, L. B., 1993. Proterozoic plutonism and regional deformation - new constraints from the southern Manzano Mountains, central New Mexico. *New Mexico Geology*, v.15, no. 3, p. 49-56.
- Bauer, P. W. and Williams, M. L., 1994. The age of Proterozoic orogenesis in New Mexico, USA. *Precambrian Research*, v. 67, p. 349-356.
- Bouillier, A-M, and Bouchez, J-L., 1982. Le quartz en rubans dans les mylonites. *Bull. Soc. Geol. Fr.*, 7 : 253-262.
- Bowring, S. A., and Karlstrom, K. E., 1990. Growth, stabilization, and reactivation of Proterozoic lithosphere in the southwestern United States. *Geology*, v. 18, p. 1203-1206.
- Condie, K. C., 1978. Geochemistry of Proterozoic granitic plutons from New Mexico. *Chemical Geology*, v. 21, p. 131-149.

- Condie, K. C., 1980. The Tijeras greenstone: evidence for depleted upper mantle beneath New Mexico during the Proterozoic. *Journal of Geology*, v. 88, p. 603-609.
- Condie, K. C., 1986. Geochemistry and tectonic setting of Early Proterozoic supracrustal rocks in the southwestern United States. *Journal of Geology*, v. 94, p. 845-864.
- Condie, K. C. and Budding, A. J., 1979. Geology and geochemistry of Precambrian rocks, central and south-central New Mexico. New Mexico Bureau of Mines Mineral Resources, Mem. 35, 59 pp.
- Ghent, E. D., Stout, M. Z., and Parrish, R. R., 1988. Determination of metamorphic pressure-temperature-time (PTt) paths. Short course on Heat, Metamorphism, and Tectonics. Mineralogical Association of Canada, p. 155-188.
- Goddard, E. N., 1966. Geologic map and sections of the Zuni Mountains flourspar district, Valencia (now Cibola) County, new Mexico. USGS Misc. geol. Investigations Map I-454, scale 1:31,680.
- Grambling, J. A., Williams, M. L., Mawer, C. K., 1988. The Proterozoic tectonic assembly of New Mexico: *Geology*, v. 16, p. 724-727.

Grambling, J. A., Williams, M. L., Smith, R. F., and Mawer, C. K., 1989.

Metamorphism and deformation of kyanite - andalusite - sillimanite and sillimanite-K-feldspar rocks in New Mexico, in Grambling, J. A., and Tewksbury, B. J., eds., Proterozoic Geology of the central and southern Rocky Mountains: Geological Society of America Special Paper 235, p. 111-118.

Grambling, J. A., and Dallmeyer, R. D., 1993. tectonic evolution of Proterozoic rocks in the Cimarron Mountains, north-central New Mexico, U. S. A. *Journal of Metamorphic Geology*, v. 11, p. 730-755.

Hames, W. E., and Bowring, S. A., 1994. An Empirical evaluation of argon diffusion geometry in muscovite. *Earth and planetary science Letters*, v. 124, p. 161-167.

Harrison, T. M., 1981. Diffusion of ^{40}Ar in hornblende: Contributions to *Mineralogy and Petrology*, v. 78, p. 324-331.

Harrison, T. M., Duncan, I., McDougall, I., 1985. Diffusion of ^{40}Ar in biotite. Temperature, pressure, and compositional effects. *Geochim Cosmochim Acta*, v. 49, 2461-2468.

- Karlstrom, K. E. and Bowring, S. A., 1988. Early Proterozoic assembly of tectonstratigraphic terranes in southwestern North America. *Journal of Geology*, v. 96, p. 561-576.
- Kottlowski, F. E., 1955. Geology of San Andres Mountains. New Mexico Geological Society, Guidebook 6th field conference, p. 136-145.
- Kottlowski, F. E., 1959. Sedimentary rocks of the San Andres Mountains. Roswell Geological Society and Society of Economic Paleontologists and Mineralogists, Guidebook 12th field conference, p. 259-277.
- Kottlowski, F. E., Flower, R. H., Thompson, M. L., and Foster, R. W., 1956. Stratigraphic studies of the San Andres Mountains, New Mexico. New Mexico Bureau of Mines and Mineral Resources, Mem. 1, 132 pp.
- Lanzirotti, A. and Williams, M. L., 1996. A more vigorous approach to dating mid-crustal processes: U/Pb dating of varied major and accessory metamorphic minerals tied to microstructural studies. *Geological Society of America, Abstracts with Programs*, v. 28, no. 7, p. 453.
- Lister, G. S. and Snoke, A. W., 1984. S-C mylonites. *Journal of Structural Geology*, v. 6, p. 617-638.

- Marcoline, J. M., 1996. Field, petrographic, and $^{40}\text{Ar}/^{39}\text{Ar}$ constraints on the tectonic history of the central Manzano mountains, central New Mexico. M. S. Thesis, New Mexico Institute of Mining and Technology, Socorro, 124 pp.
- Mawer, C. K. and Bauer, P. W., 1989. Precambrian rocks of the Zuni uplift: a summary, with new data on ductile shearing. New Mexico geological Society, Guidebook 40: p. 143-148.
- Passchier, C. W. and Simpson, C., 1986. Porphyroclast systems as kinematic indicators. *Journal of Structural Geology*, v. 8, pp. 831-843.
- Passchier, C. W. and Trouw R. A. J., 1996. *Microtectonics*. Springer-Verlag Berlin Heidelberg, Germany, 289 pp.
- Paterson, S. R. and Tobisch, O. T., 1988. Using pluton ages to date regional deformations: problems with commonly used criteria. *Geology*, v. 16, p. 1108-1111.
- Paterson, S. R., Vernon, R. W., and Tobisch, O. T., 1989. A review of the identification of magmatic and tectonic foliations in granitoids. *Journal of Structural Geology*, 11 (3): 349-363.

- Pollock, T. R., 1994. Evidence for the relative timing and character of Proterozoic deformation and metamorphism in the Ladrone Mountains, New Mexico. M. S. Thesis, New Mexico Institute of Mining and Technology, Socorro, 69 pp.
- Robertson, J. M. and Condie, K. C., 1989. Geology and geochemistry of early Proterozoic volcanic and subvolcanic rocks of the Pecos greenstone belt, Sangre de Cristo Mountains, New Mexico. New Mexico Geol. Soc. Field Conf., Guidebook 30: 165-173
- Roths, P., 1991. Geology of Proterozoic outcrops in Dead Man and Little San Nicolas canyons, southern San Andres Mountains, New Mexico. New Mexico Geol. Soc., 42nd Field Conference, p. 91-96.
- Seager, W. R., 1981. Geology of Organ Mountains and southern San Andres Mountains, New Mexico. New Mexico Bureau of Mines and Mineral Resources, Mem. 36, 97 pp.
- Simpson, C., 1985. Deformation of granitic rocks across the brittle-ductile transition. *Journal of Structural Geology*, v. 7, p. 503-511.

- Spear, F. S., 1981. An experimental study of hornblende stability and compositional variability in amphibole. *American Journal of Science*, v. 281, p. 697-734.
- Thompson, A. G., Grambling, J. A., and Dallmeyer, R. D., 1991. Proterozoic tectonic history of the Manzano Mountains, central New Mexico. *New Mexico Bureau of Mines and Mineral Resources Bulletin*, 137, p. 71-77.
- Williams, M. L., 1991. Heterogeneous deformation in a ductile fold and thrust belt: The Proterozoic structural history of the Tusas Mountains, New Mexico. *Geologic Society of America Bulletin*, v. 103, p. 171-188.
- Woodward, L. A., 1987. Geology and mineral resources of Sierra Nacimiento and vicinity, New Mexico. *New Mexico Bureau of Mines and Mineral Resources, Mem. 42*, 84 pp.
- Yardley, B. W. 1989. An introduction to Metamorphic Petrology. Zussman J. and MacKenzie, W. S., eds., John Wiley and Sons, Inc., New York, 248 pp.

Appendix A

The following is a brief summary of geochemical studies of Proterozoic rocks from south-central New Mexico with particular attention to interpretations regarding rocks of the San Andres Mountains.

Condie and Budding (1979) obtained a number of complete and partial chemical analyses which were subsequently reevaluated in later studies by Condie (1986) and Alford (1987). The mafic Proterozoic rocks of central and south-central New Mexico fall into three distinct groups: light REE depleted, flat REE patterns, and light REE enriched (Condie and Budding, 1979). This reflects differing mantle sources (K. Condie, pers. comm., 1997). Mafic igneous rocks of the San Andres Mountains fall in the "light REE enriched" group. Major and trace element data indicate that mafic rocks in the San Andres Mountains are tholeiites (Condie and Budding 1979). Alford's study included a number of geochemical analysis of metamorphosed mafic igneous, felsic volcanic, and sedimentary rocks. Metamorphosed igneous rocks include a distinctly bimodal suite of mafic rocks with tholeiitic characteristics and rhyolitic rocks with calc-alkaline trends. This is consistent with igneous rocks of Proterozoic age throughout the southwest (Condie, 1986). Alford interpreted the igneous rocks of Hembrillo Canyon to be of subduction related origin based on MORB normalized diagrams, tectonomagmatic diagrams, and a variety of discrimination diagrams. Geochemical analysis of sedimentary

rocks is shown to be consistent with the idea of deposition in a continental back-arc basin. While a number of factors including metamorphic conditions, lithology, changing tectonic setting and magma source may affect the validity of the diagrams used, the remarkable consistency shown is noteworthy.

Analysis of major and trace element compositions of siliceous metavolcanic and plutonic rocks from central and south-central New Mexico reveal three distinct groups as well (Condie and Budding, 1979). These include a high-Ca, a high-Si, and a high-K group. The high-K group is divided into low-REE and high-REE subgroups, while the high-Ca and high-Si groups exhibit enriched REE patterns. Metarhyolites from the Hembrillo Canyon area of the San Andres Mountains fall into the high-Si group. Plutonic rocks from within the current study area fall into the high-K group. The Strawberry Peak pluton exhibits high REE abundances and the Capitol Peak pluton exhibits low REE abundances, indicative of different crustal sources for these magmas (K. Condie, pers. comm., 1997). Condie and Budding (1979) interpreted these rocks to have formed in an evolving multiple rift system. Reevaluation of major and trace element trends involving a broader data base resulted in a proposed model in which deposition and emplacement occurred in a continental margin arc system or back-arc basin associated with such an arc system (Condie, 1986; Alford, 1986). These geochemical studies may characterize tectonic setting at time of deposition, but provide little information regarding the accretionary history of the area.

Appendix B

Petrographic descriptions from thin section analysis. Location of samples is shown on Plate 1.

Sample hc-2: Quartzofeldspathic schist from Hembrillo Canyon.

Mineral	%	<1mm	1-5mm	>5mm	Pre	Syn	Post	Grain Shape
quartz	40	X-----X			X-----X			sub.
feldspar	25	X-----X			X-----X			sub.
biotite	15	X-----X			X-----X			sub.
chlorite	15	X-----X				X-----X		sub.-anh.
epidote	5	X-----X				X-----X		anh.
sphene	tr.	X-----X			X-----X			elongate
muscovite	tr.	X-----X						

Foliation is defined by aligned mica and chlorite and elongate felsic grains. Lineation is defined by elongate pods of quartz that are rich in opaques as well as chlorite and biotite. Intrafolial fold in compositional layering and foliation has axial planar cleavage defined by white mica. Quartz exhibits undulose extinction, strongly sutured boundaries, and significant subgrain formation. A strong crystallographic preferred orientation is evident in felsic grains. Foliation is affected by shear band/crenulation which indicates sinistral and east-side up motion.

Sample hc-3: Metavolcanic from Hembrillo Canyon.

Mineral	%	<1mm	1-5mm	>5mm	Pre	Syn	Post	Grain Shape
quartz	40	X-----X			X-----X			sub.
epidote	25	X-----X				X-----X		sub.
plagioclase	20	X-----X			X-----X			sub.
K-feldspar	10	X-----X			X-----X			sub.
muscovite	5	X-----X				X-----X		euh.

Foliation is defined by muscovite and elongate blobs of epidote. Epidote blobs are define a lineation and are locally extended, indicating L_1 is a stretching lineation. Feldspar and quartz porphyroclasts have asymmetric tails which are mainly pressure fringes. Very little material is contributed from the central porphyroclast. Epidote locally replaces feldspar. Some core and mantle structures are evident on porphyroclasts with subgrain formation along margins. Occasional quartz ribbons show subgrain formation. Feldspar porphyroclasts are occasionally fractured.

Sample hc-5: Amphibolite from Hembrillo Canyon.

Mineral	%	<1mm	1-5mm	>5mm	Pre	Syn	Post	Grain Shape
hornblende	55	X-----X			X-----X			sub.
plagioclase	25	X-----X			X-----X			euh.-sub.
spene	10	X-----X				X---X		sub.
chlorite	5	X---X				X---X		sun.-anh.
epidote	5	X---X				X-----X		euh.-sub.
biotite	tr.	X---X				X---X		sub.
opaques	tr.	X---X			X-----X			

Foliation and strong stretching lineation defined by aligned amphibole, chlorite, and highly elongate spene. Axial; ratios of amphibole and spene are as high as 10:1. A weak asymmetry (defined by C-surfaces and shear bands) suggests sinistral and east-side-up shear. Pods of feldspar exhibit undulose extinction, sutured boundaries, and subgrain formation.

Sample hc-7: Quartzite from Hembrillo Canyon.

Mineral	%	<1mm	1-5mm	>5mm	Pre	Syn	Post	Grain Shape
quartz	95	X-----X			X-----X			sub.-anh.
muscovite	5	X---X			X-----X			sub.
magnetite	tr.	X---X			X-----X			euh.

Foliation defined by elongate quartz and bands of fine grained muscovite. Lineation defined by elongate quartz grains which are equant in section cut perpendicular to lineation. Large relict quartz grains in section perpendicular to lineation suggest that L_1 is a stretching lineation. Quartz grains exhibit strong undulose extinction and strongly sutured grain boundaries. Subgrain and new grain formation is evident. Muscovite and elongate quartz ribbons define an S-C fabric that indicates sinistral and east-side up motion.

Sample hc-8: Quartzofeldspathic white mica schist from Hembrillo Canyon.

Mineral	%	<1mm	1-5mm	>5mm	Pre	Syn	Post	Grain Shape
quartz	60	X---X			X-----X			sub.
K-feldspar	25	X---X			X-----X			sub.
muscovite	10	X---X			X-----X			sub.
biotite	5	X---X			X-----X			sub.
chlorite	tr.	X---X					X--X	anh.

Foliation defined by aligned muscovite and elongate quartz and feldspar. Quartz exhibits sutured grain boundaries and undulose extinction. Felsic grains have subgrain and new grain formation along margins. Feldspars are occasionally fractured with new grains along fractures. Both growth and deformation twins are present in feldspar. Quartz ribbons are generally monocrystalline. Foliation tends to anastomose.

Sample 108- Granite mylonite from the Boki pluton

Mineral	%	<1mm	1-5mm	>5mm	Pre	Syn	Post	Grain Shape
quartz	30	X-----X			X-----X			equant-sub.
K-feldspar	35	X-----X			X-----X			sub.-euh.
plagioclase	25	X-----X			X-----X			sub.-anh.
biotite	10	X-----X			X-----X			anh.
zircon	tr.	X---X			X---X			euh.

Foliation is defined by alternating bands of biotite and lenses of feldspar and quartz. Lineation is strong and defined by lenses of biotite. Felsic grains are strongly to moderately sutured with abundant subgrain formation. Quartz ribbons are dominantly monocrystalline although polycrystalline ribbons are present. Significant amount of myrmekite although it does not appear to be strain related (i.e. no preferred location within feldspar grains). Abundant flame perthite. Kinematic indicators include a weak S-C fabric and rare sigma porphyroclast systems. Sense of shear is sinistral with a dip slip component (east side up).

Sample 1084: Amphibolite from adjacent to the Strawberry Peak pluton.

Mineral	%	<1mm	1-5mm	>5mm	Pre	Syn	Post	Grain Shape
hornblende	90	X-----X			X-----X			sub.-euh.
plagioclase	10	X-----X			X-----X			sub.-equant
opaque	tr.	X-----X			X-----X			euh.

Foliation is defined by elongate amphibole and plagioclase. Plagioclase grains are weakly undulose with dominantly straight grain boundaries. A moderately developed granoblastic polygonal texture is evident. Amphibole occasionally overgrows opaques. In section perpendicular to lineation amphiboles are generally equant and foliation anastomoses around amphibole grains.

Sample 1255- Quartzite adjacent to Capitol Peak pluton.

Mineral	%	<1mm	1-5mm	>5mm	Pre	Syn	Post	Grain Shape
quartz	80	X-----X			X-----X			equant-sub.
plagioclase	15	X-----X			X-----X			sub.-anh.
biotite	5	X-----X			X-----X			subhedral
opaque	tr.	X-----X			X-----X			equant
zircon	tr.	X-----X			X--X			anh.-euh.

Quartz and feldspar generally equant and equigranular. Extinction is weak to moderately undulose with minor subgrain formation. Boundaries are generally straight to curved. Grain boundary bulging in places is evidence for grain boundary migration. A weak foliation is defined by occasional elongate feldspars and preferred alignment of biotite. Some alteration of feldspar to sericite. Felsic grains appear weakly annealed.

Sample 1256- Capitol Peak pluton at contact with metasediments.

Mineral	%	<1mm	1-5mm	>5mm	Pre	Syn	Post	Grain Shape
plagioclase	40	X-----X			X-----X			equant-sub.
quartz	30	X-----X			X-----X			equant-euh.
K-feldspar	25	X-----X			X-----X			equant-sub.
biotite	5	X----X			X-----X			sub.-euh.

Foliation is defined by blades of biotite. Biotite is occasionally bent into foliation. Feldspars exhibit abundant growth twins and are occasionally zoned. Some alteration of feldspar to sericite. Quartz and plagioclase exhibit moderate to strong undulose extinction. Significant fracturing of felsic grains appears to post-date ductile deformation. In zones of finer-grained material there are a large number of triple junctions with straight to curved boundaries. In coarser grained areas boundaries are more curved to lobate. Foliation appears to be combination of magmatic with a tectonic overprint.

Sample 2141- Garnet-andalusite schist From north of Ash Canyon.

Mineral	%	<1mm	1-5mm	>5mm	Pre	Syn	Post	Grain Shape
quartz	35	X-----X			X-----X			equant
plagioclase	20	X-----X			X-----X			sub.
biotite	15	X-----X			X-----X			sub.-euh.
muscovite	15	X----X			X-----X			sub.
andalusite	10		X-----X			X-----X		euh.-sub.
garnet	5		X----X				X--X	euh.-sub.

Foliation is defined by biotite and muscovite. Lineation is defined by biotite and andalusite with axial ratios up to 10-1. Quartz and feldspar are generally equant and of uniform grain size. Quartz grain boundaries are straight to weakly sutured, occasionally pinned by micas. Some triple junctions are present and felsic grains exhibit weak undulose extinction. Shadows on porphyroclasts are generally symmetrical. Garnet, biotite, and andalusite overgrow the foliation, with biotite and andalusite displaying two distinct generations of growth. Shear bands formed by mica indicate sinistral and west side up motion.

Sample 2178

Mineral	%	<1mm	1-5mm	>5mm	Pre	Syn	Post	Grain Shape
quartz	55	X-----X			X-----X			sub.
muscovite	30	X-----X			X-----X			sub.
biotite	5	X-----X				X-----X		sub.
garnet	5		X-----X			X-----X		sub.
plagioclase	5	X-----X			X-----X			sub.-anh.

Foliation is defined by alternating bands of mica rich and quartz rich layers. Lineation is defined by elongate lenses of biotite and is parallel to the direction of S_1 . Quartz grains are equidimensional with straight to weakly sutured grain boundaries and weak undulose extinction. Subgrain formation is sparse. A moderate number of triple junctions are present resulting in a granoblastic polygonal texture. A crenulation appears to be localized around garnet porphyroblasts which overgrow the foliation. Porphyroblast-crenulation relationships are asymmetrical and consistently indicate pluton-side-up motion. In views perpendicular to lineation garnet porphyroblast-foliation relationships are symmetrical.

Sample 3103: Amphibolite from south of Grandview Canyon.

Mineral	%	<1mm	1-5mm	>5mm	Pre	Syn	Post	Grain Shape
hornblende	60	X-----X			X-----X			sub.-anh.
biotite	20	X-----X			X-----X			sub.
plagioclase	10	X-----X			X-----X			sub.
epidote	5	X---X				X---X		anh.
sphene	5	X-----X			X-----X			sub.-anh.

Foliation is defined by biotite and amphibole grains. Sphene is parallel to the foliation and defines a lineation. Felsic grains are strongly undulose with sutured boundaries, varied grain size, and subgrain formation. Hornblende grains occasionally looked pulled apart with feldspar grains growing in pull apart zones. Feldspars occasionally exhibit growth twins but deformation twins are more common.

Sample 3712- Granite mylonite from eastern contact of Strawberry Peak pluton.

Mineral	%	<1mm	1-5mm	>5mm	Pre	Syn	Post	Grain Shape
quartz	40	X-----X			X-----X			sub-equant
K-feldspar	35	X-----X			X-----X			sub.
plagioclase	10	X-----X			X-----X			sub.
biotite	10	X-----X			X-----X			sub.
muscovite	5	X-----X				X-----X		sub.
opaques	tr.	X----X			X----X			
zircon	tr.	X----X			X----X			euh.

Muscovite and biotite define a foliation and tend to anastomose around elongate pods of polycrystalline quartz and large K-feldspar porphyroclasts. Lineation defined by pods of felsic grains. Quartz boundaries are straight to weakly sutured polycrystalline quartz ribbons display a granoblastic polygonal texture. Undulose extinction and subgrain formation are common. Biotite tends to form a "stepping" fabric which indicates pluton side up. A weak S-C fabric indicates the same sense of shear. S-surfaces are defined by quartz ribbons while C-surfaces are defined by biotite and muscovite.

Sample 398- Strawberry Peak granite.

Mineral	%	<1mm	1-5mm	>5mm	Pre	Syn	Post	Grain Shape
Quartz	35	X-----X					X--X	euh.-sub
K-feldspar	30	X-----X					X--X	sub.-anh.
plagioclase	20	X-----X					X--X	sub.-anh.
biotite	15	X----X					X--X	anh.
epidote	tr.	X----X					X--X	anh.

Quartz is generally equant with straight to sutured boundaries and weak undulose extinction. Some subgrain formation along margins is evident. No foliation is visible. Feldspars are anhedral, filling in interstices. Biotite clearly crystallized last, filling in remaining spaces. Texture appears magmatic with a slight tectonic overprint and no foliation development.

Sample 41416: Garnet-mica schist from adjacent to SW contact with the Strawberry Peak pluton.

Mineral	%	<1mm	1-5mm	>5mm	Pre	Syn	Post	Grain Shape
quartz	35	X-----X			X-----X			sub.
muscovite	30	X-----X			X-----X			sub.
biotite	15	X-----X			X-----X			sub.
garnet	10		X-----X			X-----X		sub.
chlorite	10	X-----X				X-----X		sub.

Foliation is defined by alternating layers of quartz and muscovite. Lamination is defined by lenses of fine grained biotite. Quartz grains are equidimensional with curved to lobate grain boundaries. Quartz grains appear to be pinned by muscovite grains. Weak to moderate undulose extinction is visible. Garnet porphyroblasts overgrow the tectonic foliation with some rotation during growth. This rotation appears to indicate sinistral and west-side-up motion. The external foliation is crenulated with an asymmetry which consistently suggests dextral and east-side-up motion. The crenulation appears to be localized at sites of garnet growth. Garnets are replaced by chlorite to varying degrees.

Sample 41420- Granite mylonite from Strawberry Peak pluton internal shear zone.

Mineral	%	<1mm	1-5mm	>5mm	Pre	Syn	Post	Grain Shape
K-feldspar	40	X-----X			X-----X			Sub.-anh.
quartz	25	X-----X			X-----X			Sub.-anh.
plagioclase	20	X-----X			X-----X			Sub.-anh.
biotite	10	X-----X			X-----X			Sub.-anh.
muscovite	5	X-----X				X-----X		euh.-sub.
zircon	tr.	X-----X			X--X			euh.
opaque	tr.	X-----X			X--X			

Foliation is defined by biotite and muscovite rich layers interspersed with lenses of quartz and feldspar. Lamination is defined by elongate pods of biotite and K-feldspar. Quartz boundaries are strongly sutured with abundant subgrain and new grain formation. Quartz exhibit undulose extinction. Feldspars exhibit both deformation and growth twins. Bands of mica tend to anastomose around polycrystalline lenses of quartz and feldspar. Muscovite and biotite are occasionally bent. Minor core and mantle structures can be seen on feldspar porphyroclasts. An S-C fabric is defined by elongate mono- and polycrystalline quartz (S-surfaces) and biotite (C-surfaces). Sense of shear is dextral and west side up. This fabric appears to be lower temperature than others in the Strawberry Peak pluton.

Sample 4142: Granite mylonite from internal shear zone, Strawberry Peak pluton.

Mineral	%	<1mm	1-5mm	>5mm	Pre	Syn	Post	Grain Shape
Quartz	45	X-----X			X-----X			sub.
K-feldspar	30	X-----X			X-----X			sub.
plagioclase	15	X-----X			X-----X			sub.
biotite	10	X-----X			X-----X			sub.

Foliation is defined by biotite and elongate lenses of polycrystalline quartz. quartz grains are moderately undulose with sutured grain boundaries and subgrain formation. Feldspars exhibit both growth and deformation twins. S-C fabrics indicate sinistral and east side up motion. S-surfaces are defined by quartz ribbons (both mono- and polycrystalline) while biotite defines C-surfaces. This appears to be lower temperature than other parts of Strawberry Peak-perhaps due to location near center of pluton.

Sample 4145: Weakly deformed granite from the Strawberry Peak pluton.

Mineral	%	<1mm	1-5mm	>5mm	Pre	Syn	Post	Grain Shape
K-feldspar	40	X-----X			X-----X			sub.
plagioclase	35	X-----X			X-----X			sub.
quartz	20	X-----X			X-----X			sub.
biotite	5	X-----X			X-----X			sub.

Biotite and slightly elongate quartz define a weak foliation. Lineation is defined by clusters of fine grained biotite. Quartz has moderate to strong undulose extinction with sutured to lobate grain boundaries. Subgrain formation is common. Feldspars contain some zones of myrmekite which do not appear to be strain controlled. Deformation twins are rare while growth twins are more common. No sense of shear indicators are evident,

Sample 6166: Quartz monzonite from the Capitol Peak pluton.

Mineral	%	<1mm	1-5mm	>5mm	Pre	Syn	Post	Grain Shape
plagioclase	40	X-----X					X---X	euh.-sub.
K-feldspar	35	X-----X					X---X	euh.-sub.
quartz	10	X-----X					X---X	euh.-sub.
biotite	15	X-----X					X---X	euh.-sub.
zircon	tr.	X---X					X---X	euh.
opaques	tr.	X---X					X---X	square

Feldspar grains are generally euhedral with concentric zoning and albite twins. Corners are generally quite sharp. Feldspar is altered to sericite. In this section no foliation is evident although field samples show well-developed magmatic foliations. Biotite occurs as infilling of interstices, indicating it crystallized last. Quartz grains are equant with straight grain boundaries and weak undulose extinction. Perthite is evident in feldspars.

Sample 9171- Felsic metavolcanic from east of Treasure Mountain

Mineral	%	<1mm	1-5mm	>5mm	Pre	Syn	Post	Grain Shape
K-feldspar	40	X-----X			X-----X			sub.
quartz	30	X-----X			X-----X			euh.-sub.
plagioclase	15	X-----X			X-----X			sub.
biotite	10	X-----X				X-----X		anh.
muscovite	5	X-----X				X-----X		anh.
opaque	tr.	X---X			X---X			
zircon	tr.	X---X			X---X			euh.

Foliation is defined by alternating bands of felsic and mafic material. Lamination defined by elongate pods of very fine grained K-feldspar and quartz. Quartz grains exhibit undulose extinction with sutured boundaries. grains tend to be elongate parallel to foliation. Subgrain formation is weak to moderate. Feldspar porphyroclasts are dominantly fractured with some new grain growth along fractures. Growth twins are present but offset due to fracturing. Deformation are also present. Feldspar porphyroclasts are occasionally boudined with quartz filling necks between boudins. Sense of shear from sigma porphyroclast systems is sinistral with a dip slip (east side up) component.

Sample 9176: Metavolcanic from east of Treasure Mountain.

Mineral	%	<1mm	1-5mm	>5mm	Pre	Syn	Post	Grain Shape
quartz	30	X-----X			X-----X			sub.
plagioclase	25	X-----X			X-----X			sub.
biotite	20	X-----X			X-----X			sub.
chlorite	10	X-----X					X---X	sub
muscovite	10	X-----X				X-----X		sub.-euh.
epidote	5	X-----X				X-----X		sub
zircon	tr.	X-----X			X---X			euh.

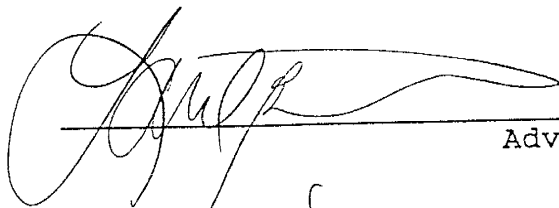
Foliation defined by alternating layers of felsic and mafic minerals. Quartz and feldspar occur in elongate of lenses of strongly undulose grains with abundant subgrain formation and sutured boundaries. Grain size is quite variable. Many feldspar porphyroclasts are fractured with new grains growing along fractures. Porphyroclast systems are dominantly symmetric. Rare asymmetric structures including sigma porphyroclast systems and minor shear bands suggest sinistral and east-side-up motion.

Sample 10217: Feldspathic mica schist crosscut by vein near Capitol Peak pluton.

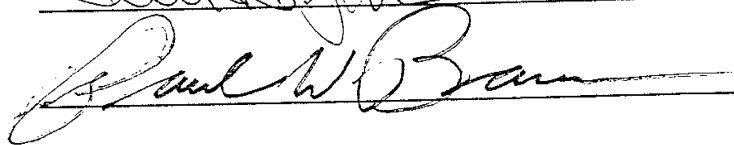
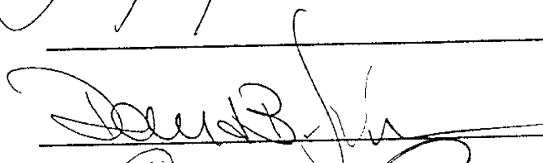
Mineral	%	<1mm	1-5mm	>5mm	Pre	Syn	Post	Grain Shape
quartz	70	X-----X			X-----X			sub.
plagioclase	15	X-----X			X-----X			sub.
muscovite	10	X-----X			X-----X			sub.
biotite	5	X-----X				X-----X		sub.
opaque	tr.	X-----X			X---X			

Foliation is defined by preferred alignment of mica. Lineation defined by micas and elongate felsic grains. Quartz and feldspar are generally equigranular with straight to curved grain boundaries and weak undulose extinction. Minor amounts of subgrain formation are evident. Muscovite occasionally pins quartz boundaries but not in sufficient amount to control fabric. Texture is granoblastic polygonal.

This document is accepted on behalf of the faculty
of the Institute by the following committee:



Adviser



August 29, 1997
Date

I release this document to New Mexico Institute of Mining and
Technology.